CHALMERS
UNIVERSITY OF TECHNOLOGY

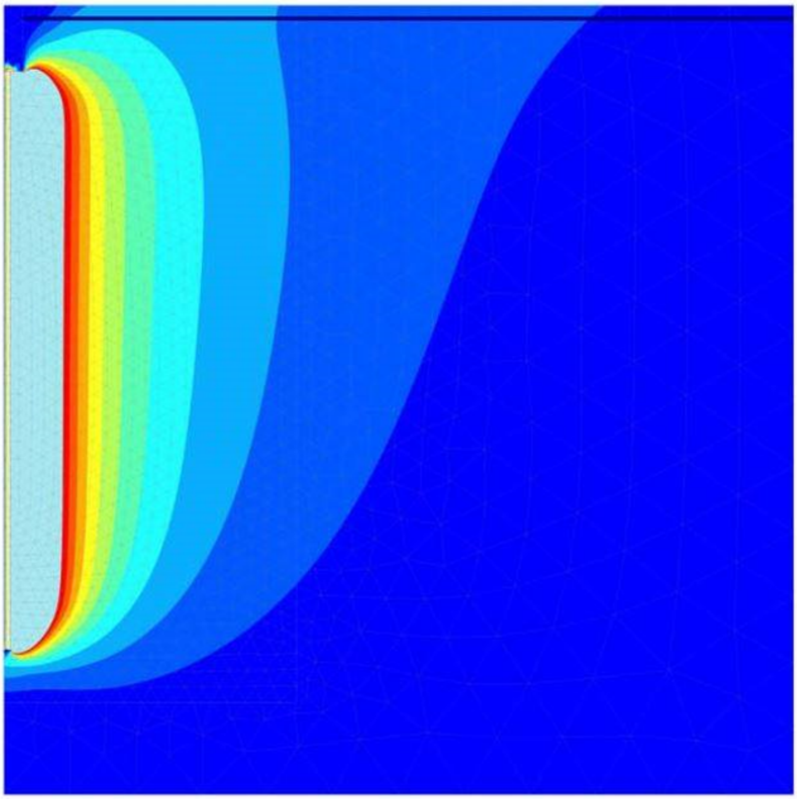

Soil displacement due to piling

Master of Science Thesis in the Master's Programme Infrastructure and Environmental Engineering

Michael Nyström

Viktor Persson

Department of Civil and Environmental Engineering
Division of GeoEngineering
CHALMERS UNIVERSITY OF TECHNOLOGY

Gothenburg, Sweden 2016
Master's Thesis BOMX02-16-101

MASTER'S THESIS BOMX02-16-101

Soil displacement due to piling

Master's Thesis in the Master's Programme Infrastructure and environmental engineering

Michael Nyström

Viktor Persson

Department of Civil and Environmental Engineering

Division of GeoEngineering

Geotechnical Engineering

CHALMERS UNIVERSITY OF TECHNOLOGY

Göteborg, Sweden 2016

Soil displacement due to piling

Master's Thesis in the Master's Programme Infrastructure and environmental engineering

MICHAEL NYSTRÖM

VIKTOR PERSSON

Examensarbete BOMX02-16-101/ Institutionen för bygg- och miljöteknik,
Chalmers tekniska högskola 2016

Department of Civil and Environmental Engineering
Division of GeoEngineering
CHALMERS UNIVERSITY OF TECHNOLOGY
SE-412 96 Göteborg
Sweden
Telephone: + 46 (0)31-772 1000

Cover:
Image output from PLAXIS finite elements software showing soil displacement from cavity expansion.

Department of Civil and Environmental Engineering. Göteborg, Sweden, 2016

Soil displacement due to piling

Master's thesis in the Master's Programme Infrastructure and environmental engineering

MICHAEL NYSTRÖM
VIKTOR PERSSON
Department of Civil and Environmental Engineering
Division of GeoEngineering
Chalmers University of Technology

ABSTRACT

Marieholmsförbindelsen is a large infrastructure project in the central of Gothenburg. The project is divided into several stages including a tunnel, two intersections and a bridge. PEAB is responsible for one of this intersections, Trafikplats Marieholm. During the construction a total amount of ca 90 kilometers piles were driven into the ground which result in soil displacements. A bridge stretches through the worksite, Partihallsförbindelsen, which have been affected by this displacements. The aim of this thesis is to investigate the horizontal soil displacement by comparing measured movements with finite element program PLAXIS 2D and analytical calculations. One foundation, G2, where investigated on the existing bridge of Partihallsförbindelsen. This foundations where affected by two pile groups, P1 and P2. The measures displacement were gained from prisms located on the foundation. Displacement below surface were gained from one inclinometer pipe. The result shows that G2 were displaced 16.5 mm at surface. Below surface the displacement increase and reach 32 mm at the depth of 10 meters then it dissipates to 28.5 mm at the depth of 20 meters were the pipe ends. Two PLAXIS 2D models were created, one plane strain model to evaluate the movement pattern around the foundation and one axisymmetric model to calculate the horizontal displacement below. Two analytical methods are used to calculate the horizontal displacement, Hellman/Rehnman method and Sagaseta's SSPM (small strain path method). The result shows that PLAXIS 2D gives the best accordance with measured displacement. SSPM shows similar result as PLAXIS 2D when looking at surface displacement while it below surface underestimate the displacement. All the methods predicts larger surface displacement than the measurements, this can be explained by the resisting force in foundation G2. Hellman/Rehnman method proves to be the least preferable method since it highly overestimate the surface displacement and gives linear displacement below surface which deviates from measurements.

Key words: Piling, Sagaseta, PLAXIS, Soil displacements, Horizontal displacements, Small strain path method

Jordundanträngning i samband med pålning

Examensarbete inom masterprogrammet Infrastructure and Environmental Engineering

MICHAEL NYSTRÖM
VIKTOR PERSSON
Institutionen för bygg- och miljöteknik
Avdelningen för Geologi och geoteknik
Geoteknik
Chalmers tekniska högskola

SAMMANFATTNING

Marieholmsförbindelsen är ett stort infrastrukturprojekt i centrala Göteborg. Projektet är uppdelat i flera steg vilket inkluderar en tunnel, två trafikplatser och en bro. PEAB är ansvariga för konstruktionen av en av dessa trafikplatser, Trafikplats Marieholm. Under konstruktionen total 80 000 – 100 000 meter pålar var slagna i marken vilket resulterade i massundanträngning. Den bro som sträcker sig genom arbetsområdet, Partihallsförbindelsen, har påverkats av dessa massundanträngningar. Målet med examensarbetet är att undersöka de horisontella massundanträngningarna genom att jämföra uppmätta rörelser med finita elementa programmet PLAXIS 2D och analytiska beräkningar. Ett fundament, G2, på Partihallsförbindelsen undersöks vilket utsätts för massundanträngningar från två pålgrupper, P1 och P2. Prismor användes för att mäta förflyttningen av fundamentet på markytan och inklinometer användes för att mäta massundanträngningen under markytan. Resultatet visar att G2 förflyttades 16.5 mm i markytan. Under markytan ökar massundanträngningen och når 32 mm på ett djup av 10 meter varefter det avtar till 28.5 mm på ett djup av 20 meter vilket också är längden på inklinometern. Två PLAXIS 2D modeller skapas, en plane strain för att utvärdera rörelsemönstret rund fundamentet och en axisymmetrisk för att beräkna de horisontella massundanträngningarna under markytan. Två analytiska metoder används, Hellman/Rehnman och Sagaseta's SSPM (small strain path method). Resultatet visar att PLAXIS 2D överensstämmer bäst med de uppmätta värdena. SSPM ger liknande resultat som PLAXIS 2D för massundanträngning vid markytan medan det underskattar massundanträngningen under markytan. Alla metoder visar högra massundanträngningar vid markytan än mätvärdena, detta kan förklaras av den mothållande kraft som uppstår för fundament G2. Hellman/Rehnman visar sig vara den metoden som avviker mest från verkligheten då den grovt överskattar massundanträngningen vid markytan och endast kan ge en linjär massundanträngning under markytan.

Contents

Preface

In this study, an investigation of the horizontal soil displacement from pile driving has been carried out. The research has been done between January 2016 and May 2016 at the Department of Civil and Environmental Engineering at Chalmers with the company PEAB Anläggning AB. The thesis was initiated by Michael Svensson and Johnny Wallgren at PEAB Grundteknik.

The study has been carried out under supervision of Dr. Jelke Dijkstra at Chalmers Institute of Technology, Mr. Michael Svensson and Mr. Johnny Wallgren at PEAB Grundteknik, who we would like to thank for their guidance. We also give our thanks to Dr. Torbjörn Edstam at Skanska who guided us through some of the analytical calculations.

Göteborg May 2016

Michael Nyström & Viktor Persson

Notations

A	Area
E’	Effective Young's modulus
E'_{50}	Effective Young’s modulus at half of the maximum pressure
V	Volume
L	Pile length
ν	Poisson's ratio
ν’	Effective Poisson’s ratio
σ	Total stress
σ’	Effective stress
τ	Shear stress
c'	Cohesion intercept
φ	Friction angle
Ψ	Angle of dilation, ratio of volumetric to shear strain

1 INTRODUCTION

Marieholmsförbindelsen is a large infrastructure project in the central of Gothenburg and is a part of Västsvenska paketet. The project is divided into four stages; Marieholmstunneln, Trafikplats Marieholm, Trafikplats Tingstad and Södra Marieholmsbron.
PEAB is responsible contractor for Trafikplats Marieholm which consists of connections, bridges, and ramps for all directions between Marieholmstunneln, Partihallsförbindelsen and E45, see Figure below.

Figure 1. Trafikplats Marieholm

The red bridge in the figure, Partihallsförbindelsen, was already constructed and during the construction of Trafikplats Marieholm PEAB installed around 80 000 – 100 000 meters of piles in the area. This pile driving resulted in extensive mass displacing that affected the structures in the proximity. During the construction, PEAB measured the foundation-, soil- and pile movement on Partihallsförbindelsen. To predict displacement PEAB did analytical calculation with the method of Sagaseta to predict the movements for the foundation, they concluded that the calculations correlated poorly compared to the on-site measured values.

1.1 Problem

When performing pile driving with mass displacing piles there is risk for environmental damage, this include damage on surrounding buildings, foundations, roads etc. which can be costly for the parties involved. To analyze and understand this process it’s of great importance to predict and plan for possible damage resulting from intensive pile driving.

1.2 Objectives

The main aim of this thesis is to investigate the surrounding displacement from extensive pile driving by comparing measured movements with finite element program PLAXIS 2D and analytical calculations. To simulate soil movement the project will include modelling in the finite element software PLAXIS 2D.

The following are the objectives:

i. To collect and analyze field measurements.
ii. To model a pile test to evaluate the soil movements from pile driving.
iii. To analytical calculate the lateral soil movement from pile driving.
iv. To compare the field measurements with the analytical- and PLAXIS results.

1.3 Scope and limitations

The amount of time to dispose is limited to one semester. Due to this, limitations has to be made, these are listed below.

There is a canal stretching through the worksite from south to north, see Figure 1. This canal will cause disturbance to the mass displacement from pile driving close to it, since the soil always takes the "easiest way". Due to this possible bridge foundation to investigate is limited.

Pile driving was performed on several location at the same time. Since the effect from one pile group will be isolated, this will limit the amount of preferable foundation to investigate.

Finite element program PLAXIS 2D can only model for one single 2D plane. By doing so the effect from different depths doesn't take into account when modelling the soil displacement in a plane strain model. To solve this an axisymmetric model can be created, however, the axisymmetric model can only calculate for one pile group at time.

2 LITERATURE REVIEW

2.1 Effects from pile driving

Pile driving in low permeable soil, such as clay and silt cause large displacement and structural disturbances which may lead to significant changes in properties of the soil and cause disruption to the surroundings, for example, foundations in is proximity (Hintze, o.a., 1997). This disruption is based on the mass displacement and the dynamic loads that the soil is exposed to during the pile driving.

When it comes to clay and silt these effects manifest itself primarily in an increased pore water pressure, reduced soil strength and large deformations. The soil mechanical effects can be divided into two categories, strength- and stiffness consequences.

The shear strength describes the magnitude of the shear stress which a soil can obtain before a failure occur. Related problems is for example the stability of different design problems, like the stability of a slope or if a foundation settles beyond its limit. The stiffness describes the magnitude of these deformations prior to the failure. Related problems is for example negative skin friction, heaving- and horizontal displacement of soil.

When piles are jacked or driven in clay, soil deformations occur due to the extra volume added in the soil. These can lead to large displacement, heave and lateral movements, see Figure below.

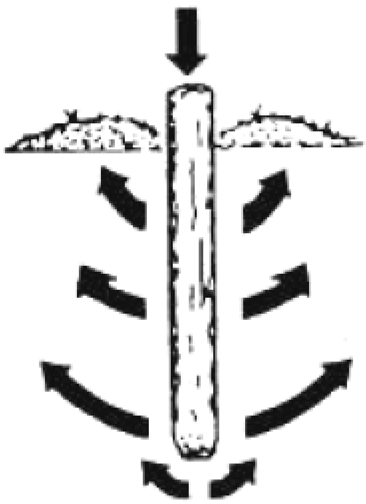

Figure 2. Soil movements due to pile driving (Hintze, o.a., 1997)

2.1.1 Undrained conditions

The undrained condition is also referred to as "constant volume", this explain the state of the impermeable soil immediately after an increase of the total stress applied and before any consolidation has started (Knappett & Craig, 2012). This means that the increment of the stress developed is carried as an increment of excess pore water pressure (i.e. no increment of effective stress). Due to low permeability in clay, seepage will take some time, resulting in an increase of pore water pressure above the static value. The static value is the initial static pore water pressure, u_s, a constant value governed by the position of the water table. The pore water pressure above the static value is called the excess of pore water pressure, u_e. The value of u_e will be equal to the value of the increment of the total vertical stress, $u_e=\Delta\sigma$. This statement only exists when the soil is laterally confined, water is incompressible and when no seepage has occurred. Therefore, after some time when water has dissipated, the pore pressure will decrease and particle rearrangement will occur which leads to an increase of effective stress. The time for dissipation depends on the permeability and compression properties.

2.1.2 Environmental impact

An important part of the work of analyzing the environmental impact is to predict the consequences on adjacent structures (Hintze, o.a., 1997). Hintze (1997) explain three main aspects to be considered when assessing the environmental impacts:

- Aesthetic and comfort –related
- Usability and functionality
- Stability and construction

The main factors that control the size of the environmental impact of the structure are:

- Type of construction/foundation
- Condition of the construction/foundation
- Duration and frequency of the impact
- Soil properties

Settlements or heave in a construction generally involves no major inconvenience as long as it takes place evenly over the construction. However, settlements and heave in the connection between the parts of the building are a problem. The subsoil below a structure is not always homogenous which result in a different degree of settlement for the structure. The settlement difference could lead to damage of the structure, the differential settlement is defined as the difference in settlement between two points in a structure. By using the distance between these two points the angular distortion can be calculated, δ/l. Bjerrum (1963) have developed a model which illustrate the limits of angular distortion, β_{max} of a structure. A specific value of angular distortion describes a problem occurring in the structure. Figure 3 shows the maximum differential settlement corresponding to the maximum settlement. Figure 4 shows the observed relationship between differential settlement and angular distortion. By combining these two figures a rough idea of the maximum angular distortion corresponding to the calculated maximum settlement of a foundation can be obtained.

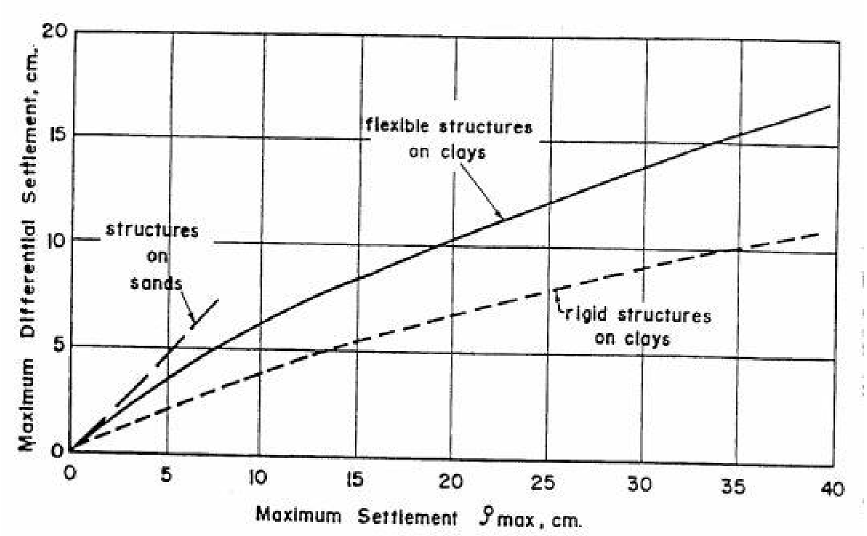

Figure 3. Envelopes of maximum observed differential settlements (Bjerrum, 1963)

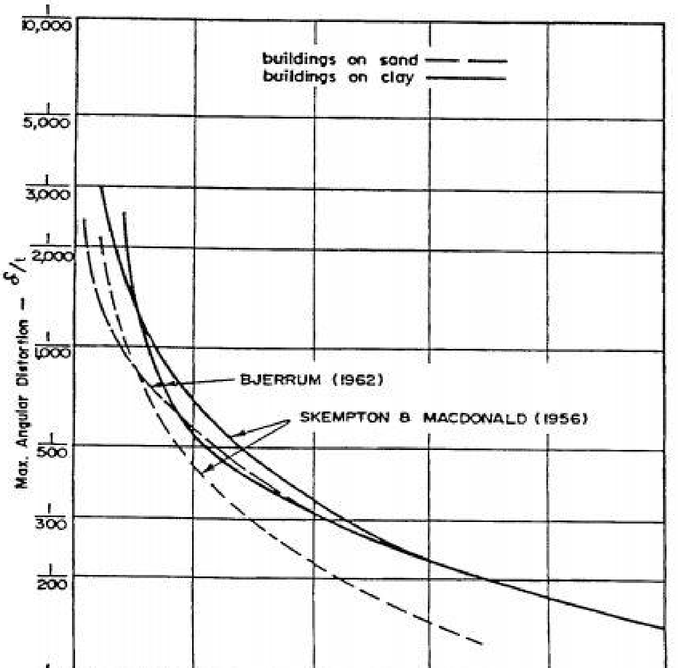

Figure 4. Observed relationship between maximum differential settlement and maximum angular distortion (Bjerrum, 1963) (Skempton & Macdonald, 1956)

However, this model perceived misleading. Since it is an ageing model and development progress of material quality and construction technics have been improved. Therefore, by today standards, the model could underestimate the limits of angular distortion for some structures.

2.1.3 Pile installation effects in clay

The change of geotechnical properties in adjacent soil due to pile installation can be summarized in three stages, see Figure 5. From left to right; installation, equalization and loading (Dijkstra, Ottolini, & van Tol, 2014). These stages illustrate the known mechanism occurring during and after pile installation. The information is based on physical experimental quantification of pile installation effects.

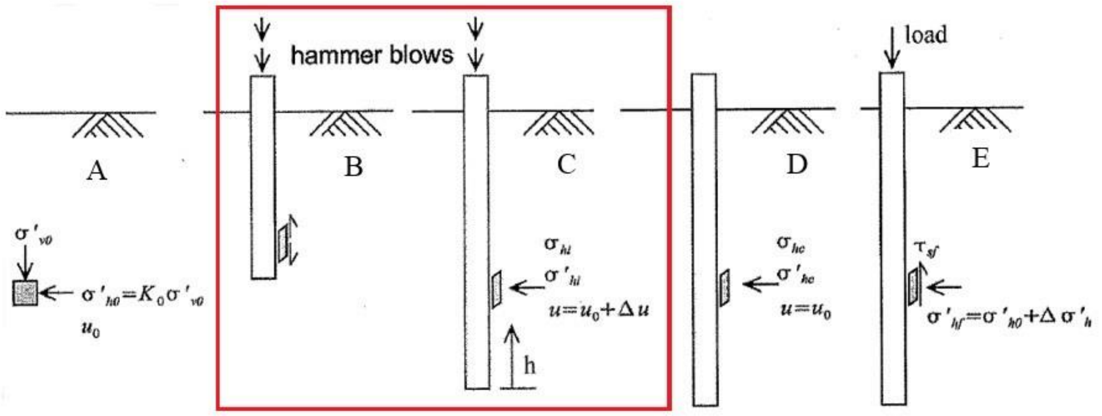

Figure 5. Installation- to loading stage (Dijkstra, Ottolini, & van Tol, 2014)

Installation stage; The pile is installed into the soil and displaces the soil outwards, perpendicular to the pile axis. Bottom of the pile the soil displaces downwards. Resulting in soil remolding and distortion. Since the process is regarded undrained condition, no volume change occurs. Therefore, when soil displaces, the increase of the total stress is accommodated by the increase of excess pore pressure.

Equalization stage; The excess pore pressure developed from the previous stage will dissipate. Resulting in a decrease of the total stress and consolidation around the pile begins. As the soil contracts the effective stress increase. This affects the void ratio that generates an increase of the soil strength. The experiment shows that the effective stress of the adjacent soil of the pile is 2-3 times higher than the shear strength.

Loading stage; In this stage, the loading is applied on the pile which transfer the load into the soil with the use of shaft friction. Hence, soil stress will increase again. Additionally, the hydraulic conductivity of the soil adjacent to the pile is altered due to the remolding and shearing of the clay during installation, also referred as the smearing zone.

The red area marked in Figure 5, illustrate the specific stages focused in this research. Since the paper isolate the impact of pile driving, only stage B and C is relevant for the displacement. Which means that in these stages, the only change in total stress is the excess pore pressure developed due the soil displacement. The temporary build up excess of pore pressure cause the soil to lose a good fraction of its shear strength.

2.1.4 Soil displacements around single pile

When driving piles into saturated clay the volume of the displaced soil is equivalent to the volume of the combined piles (Hintze, o.a., 1997). How the displaced soil volume affects the surrounding regarding horizontal displacements depends on a number of factors which mainly depends on the soil type, tension and geometric relationships within and outside the foundation area.

Physical model test at 1-g is a way to simulate the soil behavior in a laboratory, by for example, centrifuge (or shaking table) a small scale sample, similar condition of a full scale soil can be achieved. Still it’s not possible to simulate a total accurate real life scenario with a small-scale test like this. However, real scale would be an enormous project involving expensive equipment for pile driving and measurements and it’s hard to achieve accurate reproduction. Therefore a small-scale test are preferred, where the soil samples can be reproduces accurately.

There are some problem with a small-scale test that are listed below;

Low soil stress is resulting in an unrepresentative behavior and this is most common in cohesive soils because the cohesion part of the shear strength is far too high in relation to the soil stress.

The applied loads will be much smaller and therefore can't be measured accurately.

The degree of consolidation differs depending on location and soil type and would be an issue to simulate in a small-scale test.

The fact that the test isolate the effect from a single pile. When analyzing a pile group it's more complex and the effect from the surrounding driven piles doesn't take into consideration, see Chapter 2.1.5.

The center to center distance (c.t.c.) between the piles would also have an effect on the displacement. With a low c.t.c. value the displacement path would to be disturbed, especially when looking close to the pile.

With these facts taken into consideration there is reason to assume that the horizontal displacement from a small-scale test overestimates the horizontal displacement that occur. To ensure the accuracy of the displacement, test with different scale would be suitable.

In 2010, a small-scale 1-g model test was performed where the soil displacement pattern during single pile penetration was analyzed (Ni, Hird, & Guymer, 2010). In this study six areas were identified which are of importance for understanding the soil displacements caused by pile driving, see Figure below.

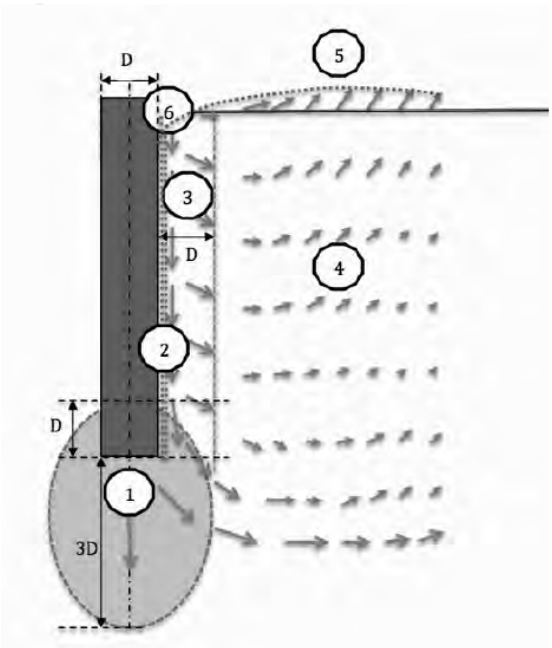

Figure 6. Schematic illustration of the displacement field and zones of disturbance during pile installation (Hintze, o.a., 1997)

Description of area 1-6:

1. Zone of disturbance below pile toe
2. Smear zone along the pile shaft
3. Zone of disturbance adjacent to the pile shaft
4. Displacement pattern adjacent to the zone of disturbance
5. Displacement at ground surface
6. Pile – soil gap

Zone 1: When penetrating a pile into the incompressible soil a bulb with high pressure is created, the bulb is approximately three times the width of the pile. As the pile penetrates into the ground this bulb moves progressively downward.

Zone 2: The smear zone is created by the relative movement between the soil and pile shaft, the structure of the soil is destroyed almost completely resulting in a reduction of the undrained shear strength. The smear zone is very thin and in sensitive clay it turns into a liquid state with low strength.

Zone 3: Within a zone of around one pile diameter a mechanical disturbance occurs. In this zone, the undrained shear strength is reduced within this zone. This zone is created from the bulb zone disturbing the soil during penetration. From this zone the soil is displaced primarily in the horizontal direction.

Zone 4: Resulting from the expansion of the pressure bulb of zone 1, this zone is subjected to resistance caused by passive earth pressure. The soil is initially displaced in the horizontal direction gradually rotated to a vertical direction.

Zone 5: In the test the surface heave reaches a maximum at the distance of 0.3 to 1.0 times the pile length.

Zone 6: During the initial driving, as a result of the downward movement of the pile toe, it's common that a gap close to the pile is created.

Regarding horizontal displacement from pile driving, Massarsch & Wersäll (2013) made the following conclusion:

"The horizontal displacement can be calculated if the pile diameter is known."
Sagaseta's Strain Path Method as well as the Cavity Expansion Method in finite element program PLAXIS.

"Already driven piles do not affect the displacement, therefore the horizontal displacement occurs symmetrically around the pole."
As mentioned earlier the c.t.c. distance and the effect on the adjacent soil from driven piles should have a mitigating effect on the displacement.

"*Pre-boring is an effective method to reduce soil displacement. However, it reduces the pile performance."*

2.1.5 Soil effects due to installation of pile group

When driving several piles in a concentrated small area it will generate higher displacement compared to a single pile. Hence, this paper is focused on water-saturated soft clay, resulting in a displacement soil volume equal to the pile volume.

A field-study regarding soil displacement due to installation of pile group was published by (Bozozuk et.al, 1978). The tests was performed in sensitive marine clay in Eastern Canada with geotechnical conditions similar to western Sweden, with a high plasticity index and water content of 60 %, which was not far from the liquid limit. The sensitivity was between 15 and 20, this is low sensitivity compare to Sweden. The following conclusion was made.

> *"Piles can only displace after they have been installed and in what direction it will displace depends on the position of the piles driven afterwards.*"
>
> *"Based on model tests and field observations it can be concluded that the lateral resistance to horizontal soil movements by already driven piles is low and can be neglected."*
>
> However, the test was performed with a c.t.c. distance of 1,5 meters. With a lower c.t.c. distance the result could differs. Since the shear strength increases with time the result could also differs when looking at long term.
>
> *"Lateral displacement of the ground surface during installation of a pile group can be complex and the direction of displacement vectors depends on the sequence of pile installation."*
>
> *"The final lateral displacements of the points surrounding the pile group are symmetrical and almost identical."*
>
> This conclusion validate the theory regarding superposition technique when calculating horizontal displacement.

2.2 Analytical methods

Two common analytical methods affecting soil movements due to pile driving in clay are; Sagaseta's "Shallow strain path method (SSPM)" and Hellman/Rehnman method.

2.2.1 Sagasetas et. al. SSPM and SPM

Sagaseta developed a method for ground movements due to pile driving in clay (Sagaseta C. , 1987). The method is using a theoretical framework called, shallow strain path method (SSPM). This method combines the previous work of steady deep penetration, called the strain path method (SPM), with methods for computing ground deformation due to the ground loss at the surface (Whittle & Sagaseta, 2001). SSPM explains displacement and strains around the pile when driven from a stress-free surface, it also explain the large strain development close to the pile that is calculated (Sagaseta C. , 1997). The SPM assumes that the deformation of the soil and strain caused by deep penetration (i.e. pile driving) in undrained soil, clay, which holds a behaviour that interpreted as fluid. Therefore, the soil is independent of the shear strength.

The calculation model is schematically illustrated in Figure 7. The model shows that a pile driven from the ground surface can be modelled with several point sources. Every point-source discharge a volume, V, in a spherical formed pattern, which leads to a field of displacement and flows around the pile, where the surrounding soil assumes to be a non-viscosity and incompressible medium within infinite full space.

The parameter, Z, correspond to the pile depth driven in the soil, Z=L. Further, a sink, S', is introduced. Which absorbs equal and opposite volume that is discharged from the point sources (i.e. V) and is located above the ground surface, Z=-L. This is done to create equilibrium concerning the vertical displacement and instead, increase the horizontal displacement with a factor of 2, at the ground surface.

A stress-free ground surface (i.e. no total/normal and shear stresses existing) is essential for SSPM and is fulfilled when the soil is assumed to be linear-elastic. By adding equal shear stress but in opposite direction, the stress-free condition at ground surface can be met. However, in order, it needs to be added to the previous shear stress factor, -2 σ_{xz}x.

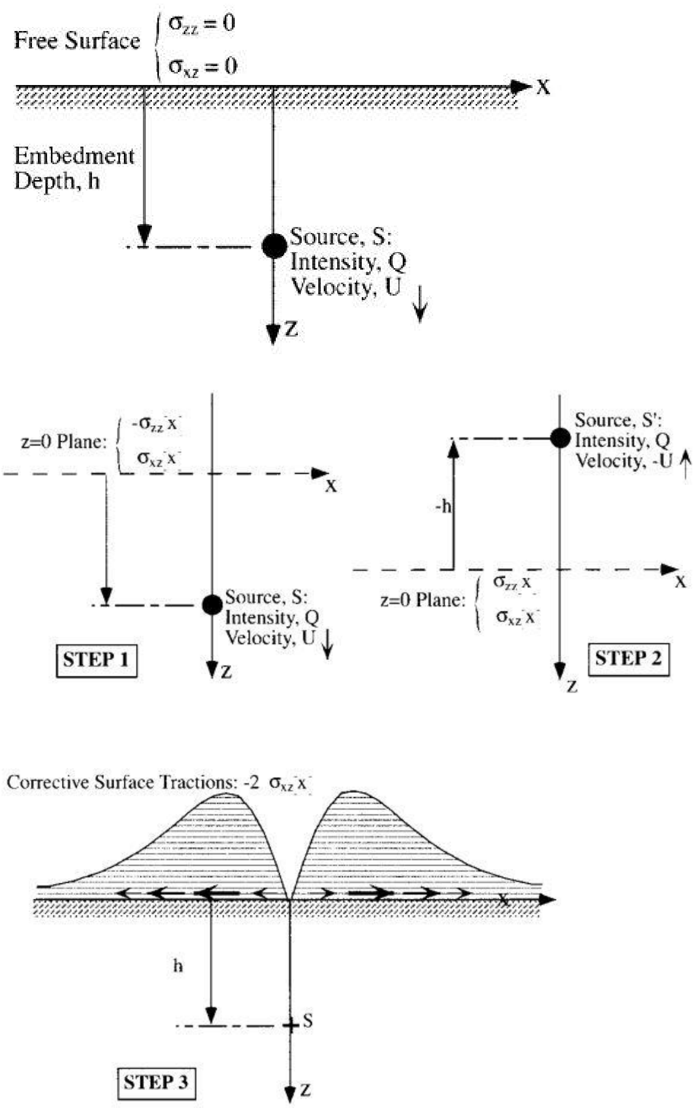

Figure 7. Conceptual Model for SSPM. (Whittle & Sagaseta, 2001)

The SSPM for calculating the vertical and horizontal movement at the surface from a single pile is presented in Equation 7 and 8.

$$\delta_r = \frac{R^2}{2} \cdot \frac{L}{r \cdot \sqrt{r^2 + L^2}} \tag{7}$$

$$\delta_v = -\frac{R^2}{2} \cdot \left(\frac{1}{r} - \frac{1}{\sqrt{r^2 + L^2}}\right) \tag{8}$$

δ_r = horizontal soil movement at the surface
δ_v = vertical soil movement at the surface
L = pile length
R = radius of pile
r = radial distance from the pile

The combined effect from one pile group can be calculated by creating a super pile including all the piles, positioned at the centrum of the pile group, this is referred as the superposition technique (Potts & Zdravkovic´, 2001). Edstam (2011) did a test to study the accuracy of this technique. In the test 16 piles were converted into one super pile and the displacement was calculated at the distance of 17.48 meters. The result showed that the accuracy when calculating with superposition technique corresponds well with single pile calculations.

There is no closed form analytical method to calculate the horizontal displacement at different depths. However, Sagaseta (1997) presented a numerical method to do so, see Figure below.

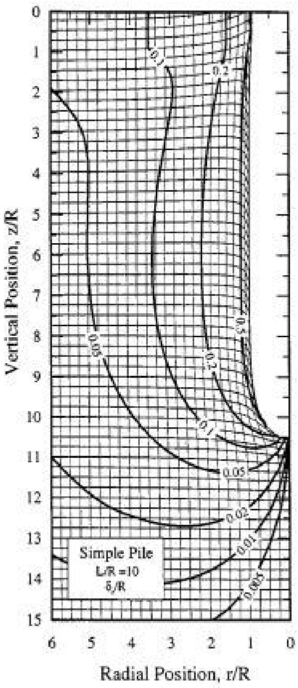

Figure 8. Horizontal displacement at different depths (Sagaseta C. , 1997)

By integrating the velocities along the particle path the displacement can be obtained, see Equation 9.

$$x(h) = x_0 + \int_0^t v_x(x,z,h)dt = x_0 + \int_0^h v_x(x,z,h)\frac{1}{U}dh \qquad (9)$$

2.2.2 Hellman/Rehnman

Hellman developed a calculation method for the assessment of the ground surface heave due to pile driving, the method is regarded as Swedish practice (Hellman, 1981). The method is based on that the surface heave is assumed to have the shape of a cone with the top cut of extending one pile length outside the piling area. In clay, this cone volume corresponds to the pile volume. The heave can be calculated according to Equation 10.

$$x = \frac{\eta(V_{pile} - V_{preboring})}{d[(\alpha+\beta)\left(\frac{1}{2}+\frac{d}{3}\right) + (\gamma+\delta)\left(\frac{b}{2}+\frac{d}{3}\right) + \frac{bl}{d}]} \tag{10}$$

x	= heaving inside the piling area
η	= factor of heaving
V_{pile}	= total volume of the driven piles
$V_{preboring}$	= total volume of the pre-boring
αx	= heaving closest to the piling area with resisting factors
βx	= heaving closest to the piling area with resisting factors
γx	= heaving closest to the piling area with resisting factors
δx	= heaving closest to the piling area with resisting factors
d	= pile length
b	= width of pile area
l	= length of pile area

Further development of the method was carried out by S-E Rehnman (Olsson & Holm, 1993). The development includes both a method to take into account the effect of surrounding buildings with different relative weight and a method to estimate the size of the horizontal displacement, see Figure 9. The heave and the horizontal displacement are assumed to be equal in size at the ground surface.

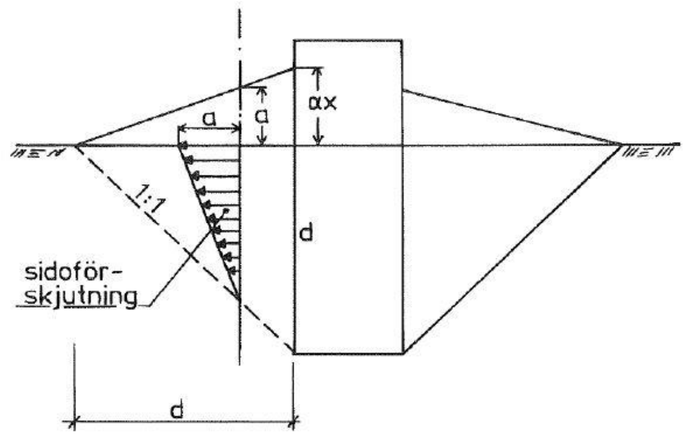

Figure 9. Horizontal movement due to piling according to Rehnman (Olsson & Holm, 1993)

2.2.3 Inclined piles

The analytical methods assume that the piles are vertical, however, in reality, many of the installed piles are driven inclined (Edstam, 2012). Edstam (2012) presented a method for analytical converting an inclined pile to vertical. By replacing an inclined pile with a combination of several vertical pile segment the effect of inclined piles can be considered, see Figure below.

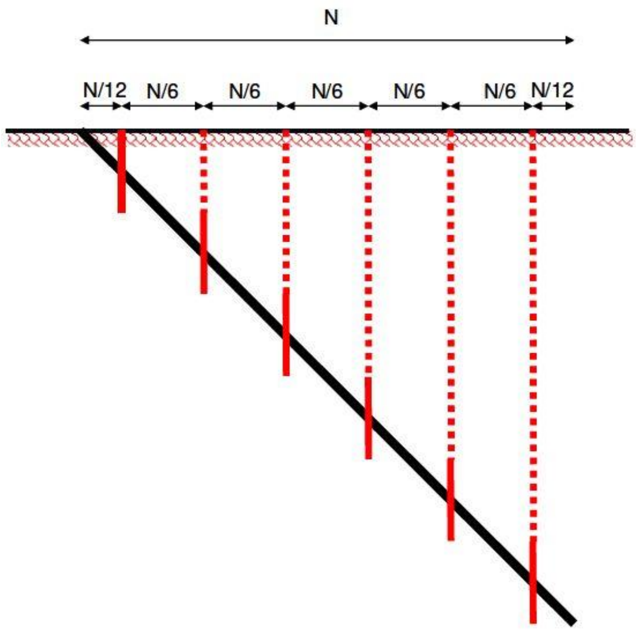

Figure 10. Inclined- to vertical -pile (Edstam, 2012)

This method requires a high number of calculation step, therefore, Edstam (2012) performed a test to see if it was possible to replace the inclined pile with one vertical. He made following conclusion; “Each inclined pile can be replaced with a vertical pile, which position coincides with the top of the inclined pile. This vertical pile has a length equal to the effective depth of the inclined pile”

However some scepticism need to be mentioned regarding this method. The volume of the combined vertical piles is less than the total volume of the inclined pile, the displaced volumes will therefore be less than in reality. The test Edstam performed when he looked at the displacement was at the distance of 17.5 meters, shorter distance would result in greater uncertainty especially when looking below the surface.

2.3 Cavity expansion

There is no function in PLAXIS 2D to model the installation of piles. However, by expanding a cylindrical cavity it’s possible to simulate the horizontal displacement from pile driving (Sheil et.al. 2015). This method is called Cavity Expansion Method (CEM). Studies have been performed by using CEM for different purposes, see below.

> Butterfield and Banerjee (1970) did the first study involving expansion of a cylindrical cavity from zero radius to a finite radius. In the study they used the method to evaluate the pore water pressures developed due to pile driving in saturated soils, their dissipation with time and the resulting time dependent variation of pile load carrying capacity. They did comparison with published data from field measurements and concluded that the theoretical results show encouraging agreement.
>
> Lehane and Gill (2004) did a study to provide accurate measurements of the soil displacement path during undrained installation of a penetrometer. The study includes measurement during the installation of six separate closed-ended pipe piles in clay and reported good agreement between CEM results and measured radial displacements.

Sheil et al. (2015) presented a new simplified method in order to consider the effect from the installation of a pile group. The method is referred to as Volumetric Tunnel Expansion (VTE) and involves the expansion of tunnels in a plane strain model in PLAXIS 2D. This method distinguishing from the conventional CEM which is using an axisymmetric model. They concluded that this method showed good agreement to traditional CEM prediction in addition to measured field data.

The publications above are focused on displacement of single piles and cavity expansion in general. Reason for this could be that the superposition technique gives inaccurate values for displacement close to the pile group. Since the focus in this study is rather the effects farther away from the piles, CEM and VTE should be suitable. However, a study focusing on the accuracy between superposition and single pile displacement in FEM would eliminate the uncertainty.

2.4 Field measurements

Field measurements during piling are used to observe movements in surrounding soil and nearby structures. This an important part of the construction phase so that counter measures can be applied if excessive movements occur in the structure.

2.4.1 Inclinometer

Inclinometer is a common method used for measuring soil movements (Stark & Choi, 2007). The tool measure the geomagnetic inclination (i.e. the inclination to the horizontal or vertical plane, an objects inclination in relative to the gravity). The measurements begin with an inclinometer-pipe bored into the soil to desired depth. Due to the low stiffness of the pipe, it will follow the movement of the soil. The inclinometer instrument is inserted into the pipe and as it moves along it register the pipes inclination and transfer the data to a software that convert the values to horizontal displacement. Inclinometer can also be used for measurements of concrete piles, by implementing an inclinometer-pipe into the pile the pile straightness and twist can be measured. There is also possible to measure the pile deformation during the pile driving. Figure 11 illustrates the principles of inclinometer configuration of inclinometer equipment's and Figure 12 illustration of inclinometer operation.

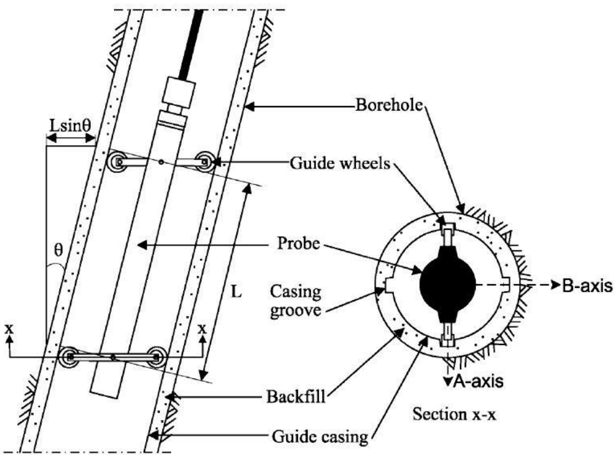

Figure 11. Principle of inclinometer (Stark & Choi, 2007)

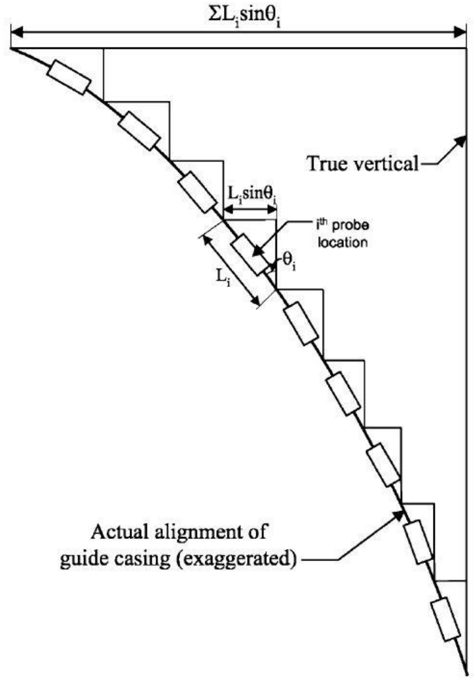

Figure 12. Illustration of inclinometer operation (Stark & Choi, 2007)

The accuracy according to product suppliers is ±2mm over 25 meters. However, there are uncertainties regarding the accuracy which usually is not mentioned by the suppliers. The precision depends on several factors such as the readout system, cable, and probe, quality of the casing and the design of the sensor. Stark (2007) presented a paper that presents some guidelines for understanding the use of inclinometers. In the paper he mention uncertainties regarding the accuracy which are listed below.

The inclinometer need to be fixed at a point with zero displacement, if not the inclinometer will not capture the total amount of movement.

The same probe and electrical cable used for the zero reading should be used for subsequent readings so all of the readings are comparable to the zero reading.

The pipe need to be inserted with the same orientation of the instrument and require successive readings at the same depth in the casing.

If possible, it's preferable that the same person performs all of the readings so the results do not have any unwarranted differences from the zero reading.

These consistencies are of create importance since the direction-, rate- and magnitude of movement are derived from the difference between the zero and subsequent readings. Therefore, using the same equipment and if possible the same operator is critical to make the measurement accurate.

2.4.2 Total-station

The most common method of measuring lengths is to use an EDM instrument (electro-optical distance measuring instruments) (Leica-Geosystems, 2013). These instruments are integrated with a Theodolite in a so-called Total-station, see Figure 13. A total-station measures the vertical angle, horizontal angle and slope distance against an optical reflective prism with and accuracy of about 1.5 millimeters over a distance of up to 1500 meters. This method could be used to measure movements of foundations, like in this case, bridge foundation movements due to additional piling.

Figure 13. Total-station; Leica TM30. (Leica-Geosystems, 2013)

3 METHODOLOGY

3.1 Description of the area

3.1.1 Partihallsförbindelsen

Partihallsförbindelsen was completed in 2011 and is an 1150 meters long four-lane road bridge extending from E20 at Åsnäsmotet to a new intersection connecting to E45 at Marieholm. The bridge was already constructed when the piling for the intersection of Marieholm began. The consisting bridge foundations of Partihallsförbindelsen are located close to the piling area. Measurements from the test site show that these foundations have been affected in the horizontal direction from the intensive piling.

During the construction, PEAB measured the foundation-, soil- and pile movement on Partihallsförbindelsen, Appendix 1 shows these different types of measurements.

3.1.2 Test site

The pile foundation, G2, which will be analyzed is being exposed from pile groups P1 and P2, the blue lines illustrate the project which is being constructed, see Figure 14.

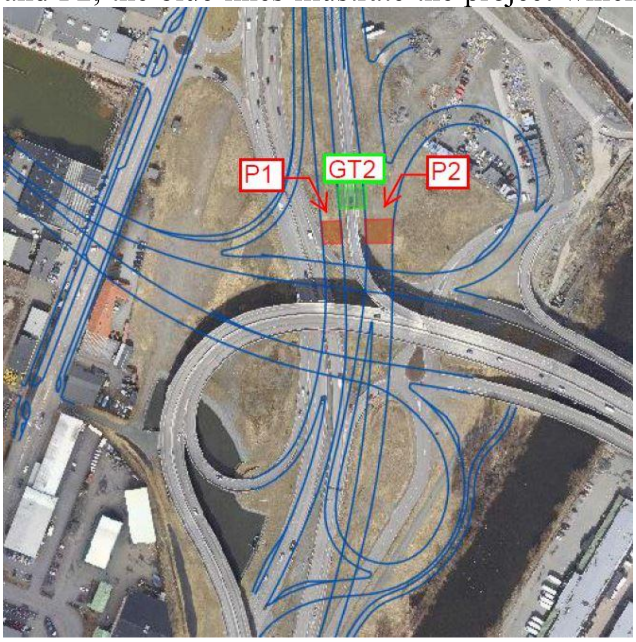

Figure 14. Exposed foundation and pile groups

Foundation G2 have free movability in a south-north direction, however, this movement is limited. If the horizontal displacement of the foundation exceeds this distance undesired tensile stress will appear in the construction.

P1 consist of 35 piles with an average length of 45 meters and P2 consist of 41 piles with an average length of 52 meters, see Appendix 2. Figure 15 shows the distance and orientation of the pile groups in relation to G2 foundation. P1 holds an average c.t.c distance of 2.6 meters and P2 holds an average c.t.c distance of 2.8 meters. Pre-boring is done for specific piles to a depth of 12 meters. P1 and P2 are vertical driven embankment piles, see appendix 10.

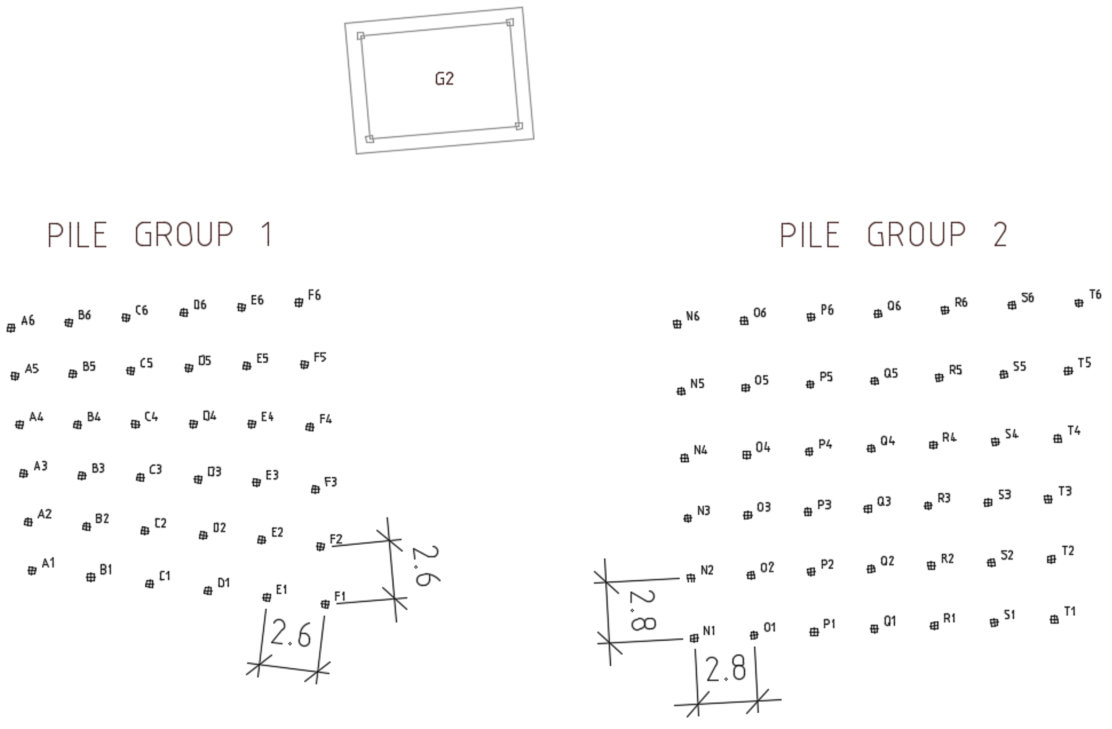

Figure 15. Plan view, scale 1:200.

3.1.3 Topography and soil conditions

The ground surface is relatively flat with levels that mainly varies between +10 in the south location and +12.5 in the north location. The area consists of existing roads, E45, Partihallsförbindelsen and buildings. Vegetation in the area consists mostly of spontaneously established areas of grass, small extent of bushes and minor trees occurs and some larger trees. The area has been filled in stages through the nineteenth century from the original ground surface. Soil layers occur in order; dry crust/fill, clay, moraine, bedrock. A stream is located in the south region and stretches from south to north-east with an average depth of 5 meters.

3.2 Collection of field measurements

Two types of measurements have been analyzed for the G2 foundation, see Figure 16. The measure points (prisms) and the inclinometer measurements are automatically measured once a day by a total station. Inclinometer- and prism measurements are collected and stored with the softwares Teroc and Projectnav.

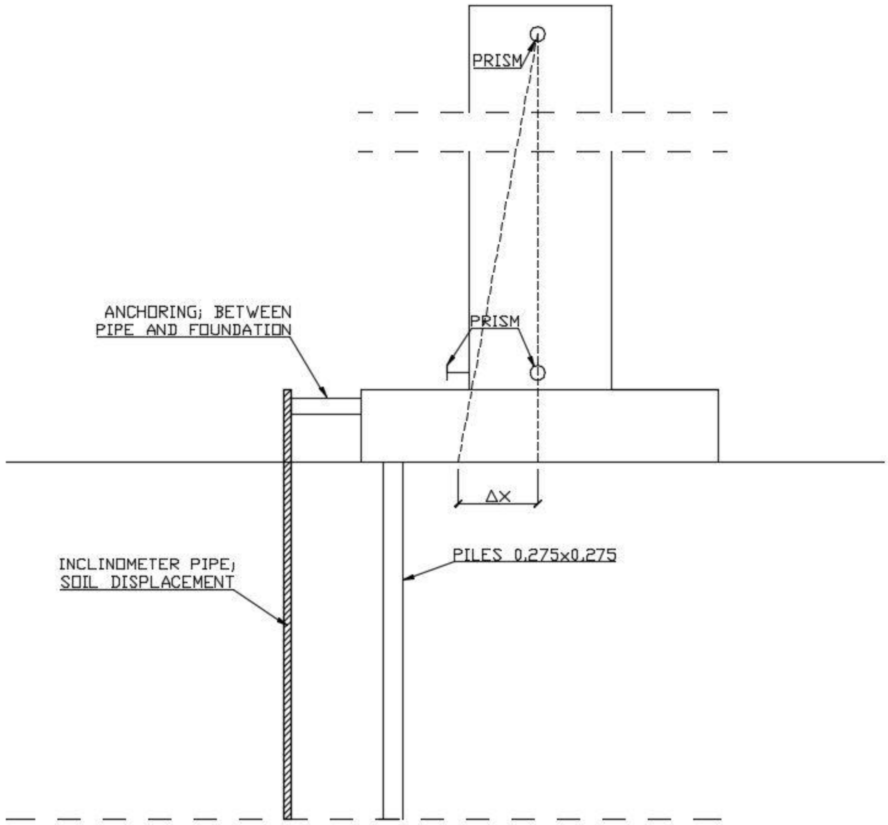

Figure 16. Profile view of G2 foundation, scale 1:100.

3.2.1 Prism

Two prisms are located on G2 foundation, one lower close to the foundation footing and one higher close to the connection between bridge-foundation. By comparing the horizontal displacement for each prism it's possible to draw two conclusions.

> Firstly, if the difference in horizontal movement for each prism is known the horizontal displacement, Δx, at the surface can be calculated, see Figure 16. For G2 foundation the upper horizontal movement is measured to 22 mm and the lower to 20 mm, this gives the footing a total horizontal displacement of 19.5 mm.
>
> Secondly, if the upper prism have a lower displacement than the lower prism it will result in tension of the bridge-foundation connection. For G2 foundation the displacement for these prism are similar, indicating that there is no tension generated by additional piling.

By only focusing on measurements for the specific time period when the driving of pile group 1 and 2 took place it's possible to isolate the effect on the foundation from these two pile groups, see Figure 17.

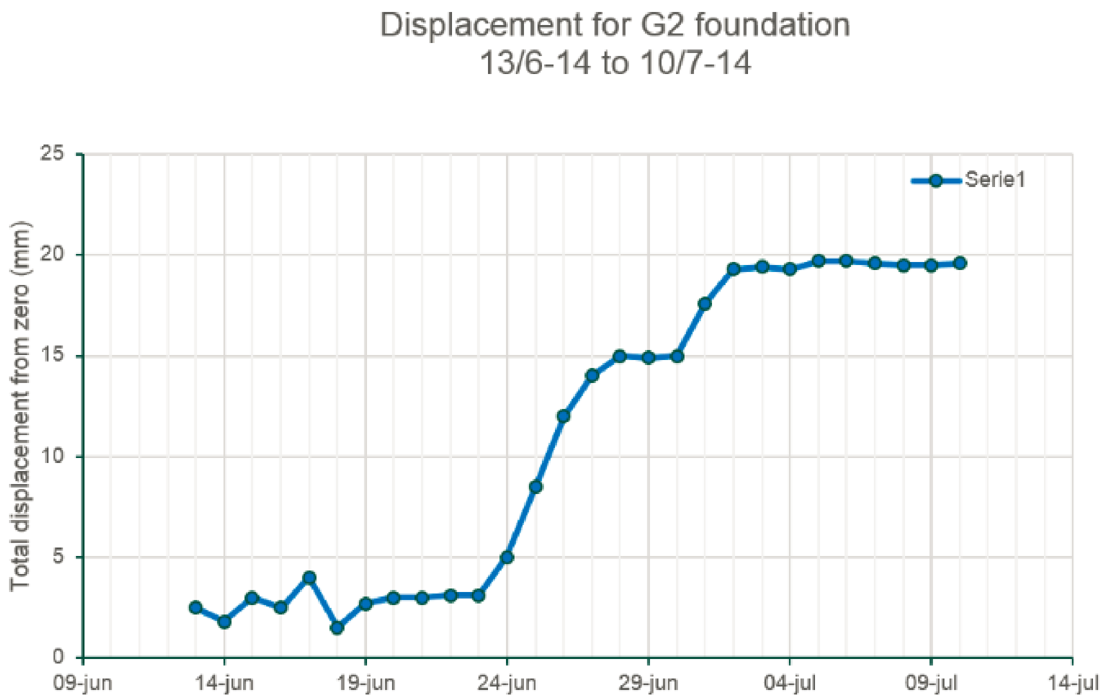

Figure 17. Horizontal displacement of G2 footing.

The figure also shows that low movement occur before and after piling. This gives an correct isolation of the time period where the foundation only are affected by the additional piling, pile groups P1 and P2.

Displacement of the higher and lower prism are interpolated to get the footing displacement of the foundation, see Table 1.

Table 1. Horizontal displacement for G2 foundation

Displacement [mm]	16/6-14	7/7-14	Change
Higher prism	3	22	+19
Lower prism	3	20	+17
Footing	3	19,5	+16.5

3.2.2 Inclinometer

The inclinometer pipe goes to the depth of 20 meters. Since the pipe is fixed at the foundation the inclinometer shows a value of zero displacement at the top, therefore the total horizontal displacement for the foundation has to be added to the inclinometer values to get the correct horizontal displacement of the soil.

The inclinometer reference point starts at 20 mm, due to foundation movement, see Table 1. Figure 18 shows the inclinometer measurements of the foundation.

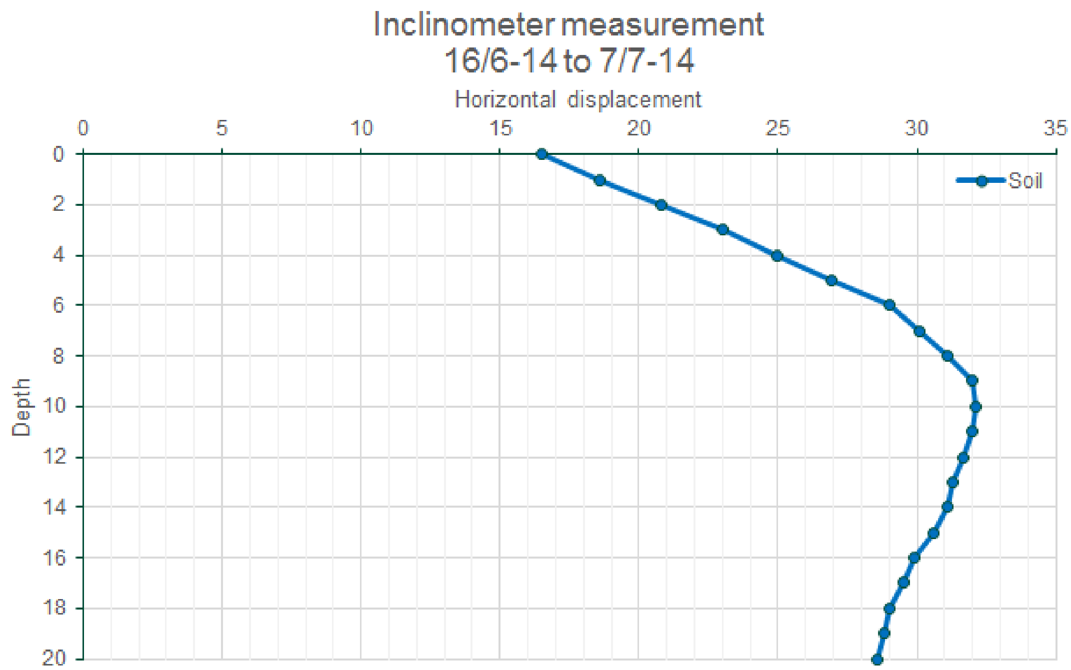

Figure 18. Soil displacement, G2

Measurement results for the inclinometer pipe shows that the underlying soil has a larger horizontal displacement than the foundation. This indicates that there is a resisting force for the underlying pile construction.

3.2.3 Uncertainty of measurements

There are a few uncertainties regarding the accuracy of the measurements. First, since the total station is fixed at one of the bridge foundation there is a risk that the foundation has been displaced as well. The total station use reference points to calculate its location, the reference points have a maximum distance of 300 meters. These reference points is located at houses and structures which also moves with time which will lead to errors in the measurements. This could lead to the fact that either more or less displacement is registered for the G2 foundation. However, the total station is calibrated to alert when the reference points differ more than 2 mm, and when this happens the reference point will not be used. These reference point are recalibrated every 6 months to eliminate large faults. Assessments from the work site show that the maximum error the total station register is 2-3 mm.

Except the uncertainties mentioned in the literature study there is some site specific uncertainty regarding the inclinometer measurement. The low stiffness of the inclinometer pipe makes it sensitive during and after the installation process. One large source of error occurs at the top near the surface where the inclinometer pipe is attached to the foundation. This attachment point is set to the reference point and is assumed to be totally fixed, however, in reality, this is not the case. The optimal attachment would be to weld the pipe to the foundation with some kind of steel structure. In our case, however, the inclinometer pipe is attached to the foundation with a wooden structure which is weaker and more sensitive to the weight of the soil around it. Due to this, the reference point could move and register larger soil movement than actually occurs. Since the attachment is below the surface we cannot see if this is the case for our foundation, however, it’s important to take this into account when evaluating the results.

3.3 Superposition technique

Edstam (2011) used the maximum amount of piles to 16 when calculating with the superposition technique, using SSPM. Therefore, in this section, a test will be performed with the purpose to test if it’s possible to use more piles in the technique. The test is divided into five stages, for each stage different amount of piles is used for the super pile. A point 15 meters from centrum with a c.t.c. distance of 2.8 meters is used to compare the displacement, see Figure 19. The result will be compared with single pile calculation where the sum of each pile displacement is accumulated. The calculations is presented in Appendix 4.

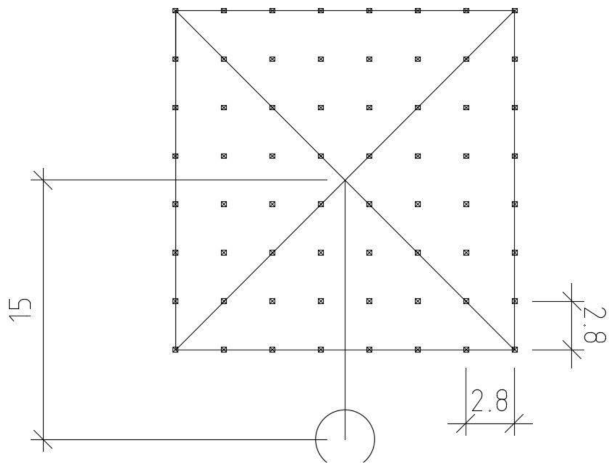

Figure 19. Plan view of the superposition geometry, scale 1:200.

3.4 PLAXIS

PLAXIS is a software based on the Finite Element Method (FEM). The FEM is a computational process that gives approximate solutions to a boundary value problem. The mathematical calculations performed are approximated by a series of algebraic equations in a region of interest.

There are several different material model implemented in PLAXIS, Mohr-Coulomb is one of them and is used for modelling in this paper. Mohr-Coulomb possesses an elastic perfectly-plastic behavior (Knappett & Craig, 2012).

The fact that PLAXIS 2D only calculate in a two dimensional plane makes it problematic to simulate the total displacement from a real life scenario. As presented in the literature review the total horizontal displacement at a specific depth is affected by the displacement at every depth, see Figure 6. Two PLAXIS models will be created, one plane strain model and one axisymmetric model. The plane strain model will simulate the horizontal soil movement around a foundation at a horizontal cross section. The axisymmetric model will simulate the horizontal soil movement below at a vertical cross section.

3.4.1 Determination of model parameters

The strength and stiffness parameters that are used depends on what condition the model possess, drained or undrained. Stiffness and strength for drained behaviour are defined in terms of effective properties. For undrained behaviour, there is three different methods, A, B and C.

Method A; analysis in terms of effective stresses.
Effective strength parameters; c', φ', ψ'
Effective stiffness parameters; E', v'

Method B; analysis in terms of effective stresses.
Total strength parameters; $c = c_u, \varphi = 0, \psi = 0$
Effective stiffness parameters; E', v'

Method C; analysis in terms of total stresses
Total strength parameters; $c = c_u, \varphi = 0, \psi = 0$
Total stiffness parameters; $E_u, v_u = 0.495$

The material model used in this paper is Method B. The Table below shows the input model parameters.

Table 2. Model parameters for PLAXIS

Model parameters	
c_u	13 kPa +1.2 kPa/m
φ	0 °
ψ	0 °
E'_{50}	4250 kPa +125 kPa/m
v'	0.35
γ	16.5 kN/m^3
K_0	0.6

The effective stiffness modulus E'_{50} is chosen since relatively large strains are expected, E'_{50} is evaluated from active drained triaxial tests. To obtain fully incompressible soil v_u is equal to 0.5. However, this value cannot be used because it would result in an infinite value of bulk modulus. In order to avoid numerical problems, v_u is by default taken as 0.495. To ensure that the skeleton of the soil is much more compressible than the pore water, v' is therefore set to 0.35. The dilatancy- and friction angle are both set to zero due to the fine grained soil and low permeability. The undrained shear strength c_u is evaluated from CPT-test. K_0 is the relation between the horizontal- and vertical in-situ stresses. More details about the determination of soil parameters is presented in Appendix 5.

3.4.2 Plane strain model

Expanding the volume of an elastic material will cause horizontal movement for the surrounding soil, the model will have two volume expansion representing each pile group, see Figure 20. To consider a horizontal plan view the y-direction is no longer vertical but instead on a horizontal plane normal to x-direction. To ensure symmetry between the x- and y-axis, the lateral earth pressure, *K*, is set to 1. This gives the stress relation, $\sigma'_{xx} = \sigma'_{yy}$. PLAXIS use gravitation that creates stress in the y-direction. However, to ignore this the unit weight of the materials is set to zero, another way to ignore gradient stress due to gravitation is to set the sum weight to zero founded in the phase properties. To represent the horizontal stresses at specific depth a spread load is applied on the top- and right side boundaries.

The steps taken to set up the model are as follows:

1. Set up geometry of the model.

Regarding the expanding pile groups an elastic 'dummy material' is chosen. The foundation is represented by plates with a node to node anchor, by specifying stiffness of the anchor it's possible to simulate movement in the foundation. The figure below shows the geometry for the model.

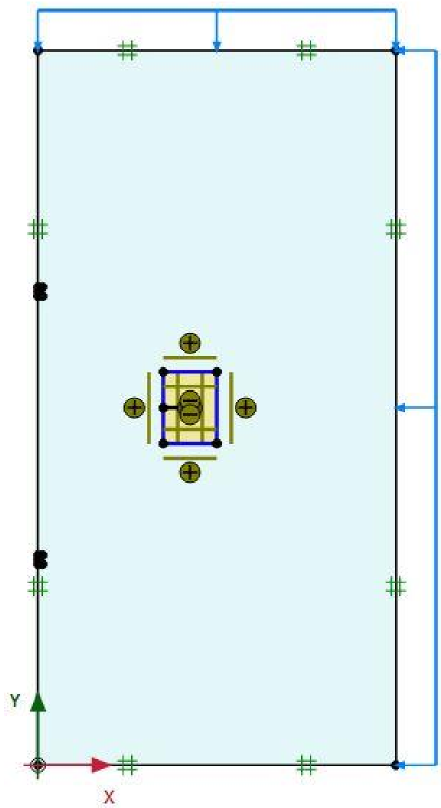

Figure 20. Geometry of the model

2. Define the mesh.

Finer mesh, with a coarseness of 0.25 concentrated around the expanded volumes, since this is the area of greatest interest. For the surrounding soil, a coarseness of 1 is used, to decrease the computational time. The mesh is displayed in the figure below, the refined mesh is inside the blue rectangle.

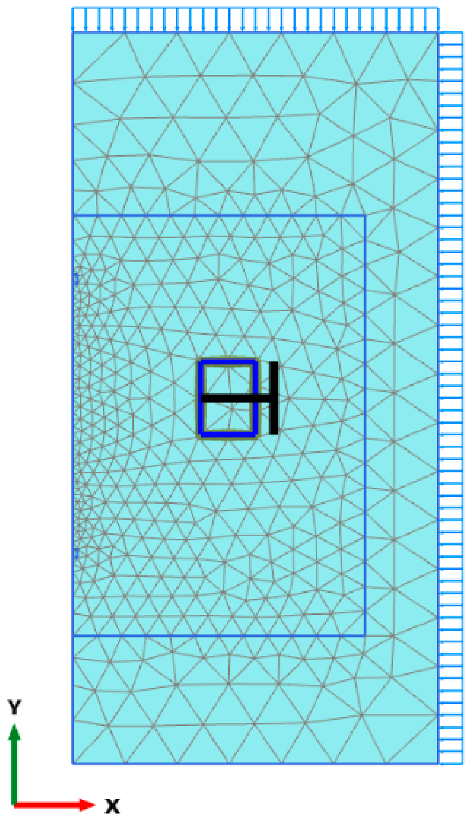

Figure 21. Mesh generation

3. Calculation is divided into three main phases:

Phase 1: Activating the spread loads on top- and right side boundaries.

Phase 2: Deactivating the loads and fix the model boundaries in normal direction, this is done in order to keep the stresses.

Phase 3: Volume expansion of the two pile groups, this value is set equal to the total volume for each pile group. If the volume expansion is large this step can be divided into several phases.

The output result is presented in Appendix 8.

3.4.3 Axisymmetric model

In the axisymmetric model the y-axis will represent the depth and the x-axis the radial distance from the pile. The model will have one cavity expansion representing the pile group. However, since we have two pile groups the model will be set up two times each representing one pile group.

The steps taken to set up the model are as follows:

1. Set up geometry of the model.

Material model is set to Mohr-Coulomb (Undrained B). Regarding the expanding pile groups an elastic 'dummy material' is chosen. There will be no foundation in this model since we only will look at the displacement in the spoil at a specific distance. The Figure below shows the geometry for the model.

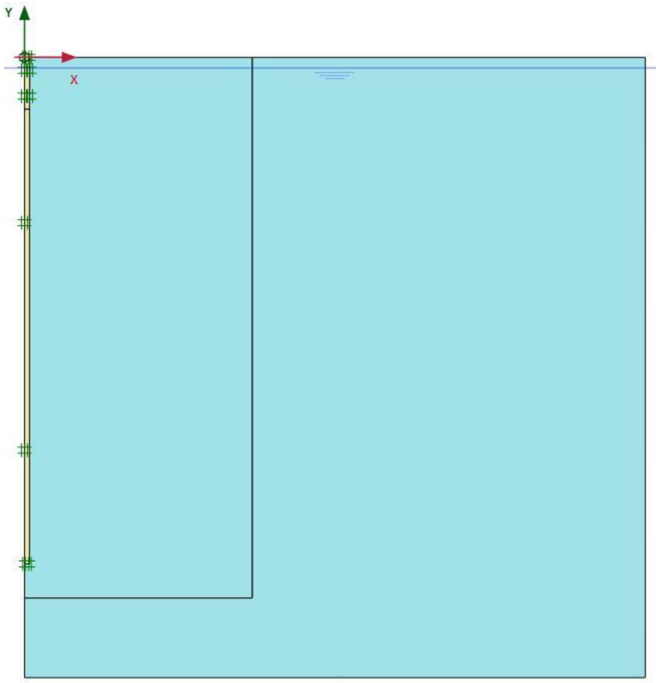

Figure 22. Geometry of the model

2. Define the mesh.

Finer mesh, with a coarseness of 0.25 are concentrated around the expanded volumes to the distance where the displacement will be plotted. For the surrounding soil, a coarseness of 1 is used, to decrease the computational time. The mesh is displayed in the Figure below, the refined mesh is inside the blue rectangle.

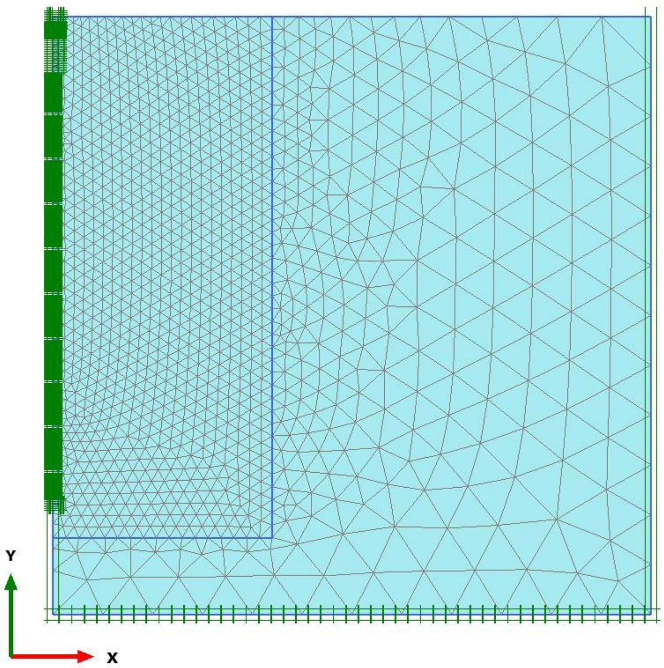

Figure 23. Mesh generation

3. Calculation in one phase:

Phase 1: Volume expansion of the pile group, this value is set equal to the total volume for each pile group. If the volume expansion is large this step can be divided into several phases.

Displacement from each pile group is presented in Appendix 9. The displacement from each pile group will result in vectors at different depths. By using vector addition the total displacement at a specific distance can be calculated.

3.5 Analytical calculations

In this section the methodology for calculating soil displacement with the methods SSPM and Hellman/Rehnman is explained. For both analytical methods the average length of the piles is used, this is done to avoid splitting up the pile groups.

As described in the literature study, when calculating with the method of SSPM, P1 and P2 needs to be converted into super-piles, this procedure is presented below.

Two super-piles is created, S1 and S2, each representing P1 and P2, see Figure 24. Each super-pile is places at the center of the square pile group it replaces, while its cross-sectional area is equal to the sum of the cross sectional area of all the included piles. This gives a cross sectional area of 2.72 m^2 for S1 and 3.18 m^2 for S2.

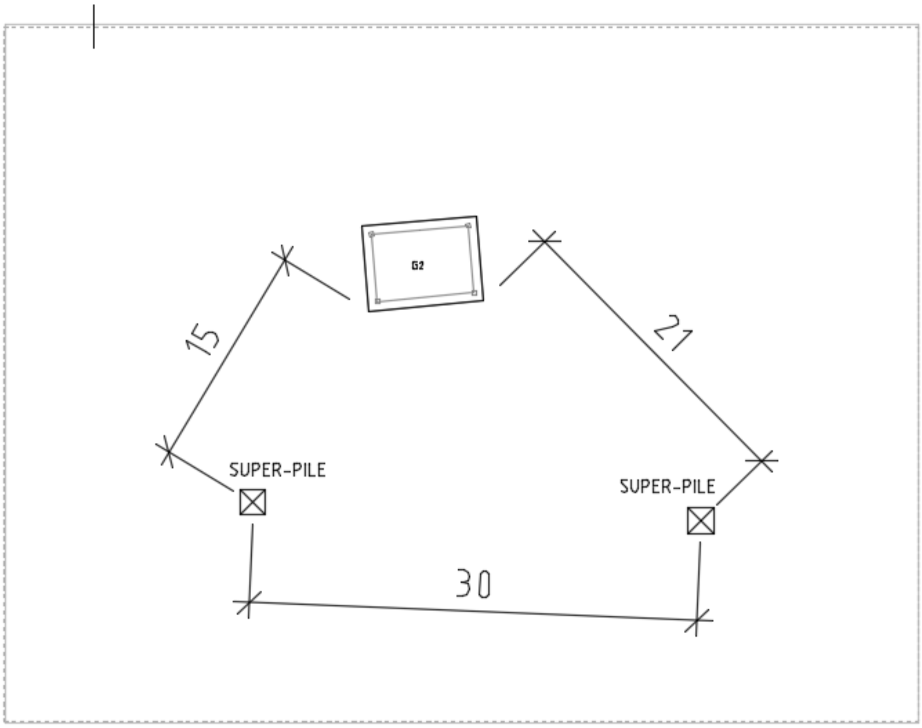

Figure 24. Position of super-piles

Pre-boring is done for 44% of the piles in P1 and 52% of the piles in P2, see Appendix 2. The effect of the pre-boring is considered by creating two negative super-piles, one for P1 and one for P2. The cross-sectional area for each super-pile is equal to S1 and S2, but with the depth to 12 meters.

When the position and geometry of the super-piles is known we can now calculate the horizontal displacement at surface, Equation 7 is used. When calculating the horizontal displacement below the surface the numerical method described in Chapter 2.2.1. is used, the calculations are described in Appendix 6.

The displacement from the two pile groups is resulting in two vectors, by using vector addition we can calculate the vector resultant. The vector sum in our case is the total horizontal displacement and direction for foundation G2. These calculations is shown in Appendix 6.

For Hellman/Rehnman Equation 9 is used, this method use the dimension for the whole pile group instead of the superposition technique. The first step is to convert the two pile groups into squares, see Figure 25.

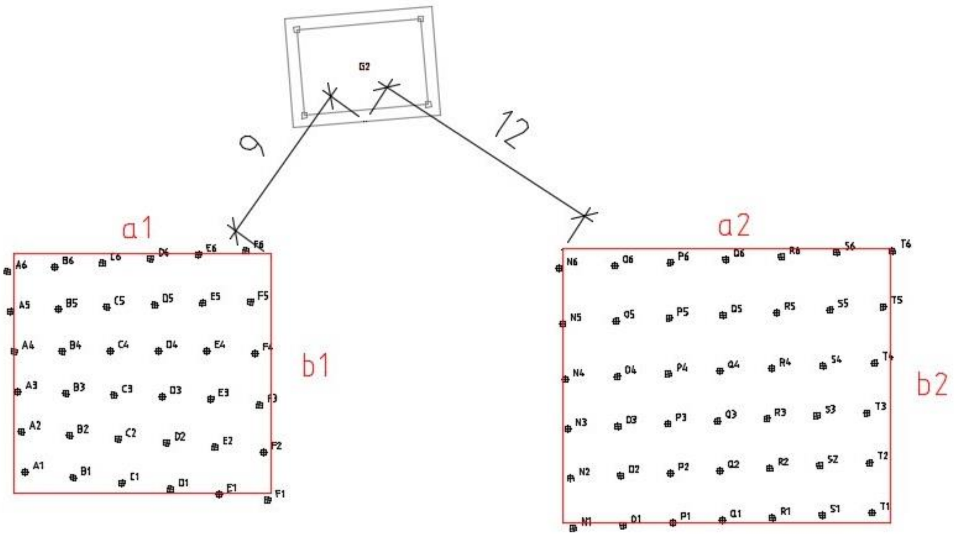

Figure 25. Geometry for Hellman/Rehnman

Hellman/Rehnman assumes a linear movement below the surface, this is shown in Figure 9. The effect from the pre-boring can be ignored when the distance to the displacement point exceeds the depth for the pre-boring, this is the case for pile-group 2. There is no surrounding buildings close to the foundation, so this effect can be ignored. The displacement at the distance x can now be calculated according to Equation 10.

$$\delta_v = \delta_r = \frac{\Sigma V_{pile}}{\left(\frac{4}{3} \cdot L_{pile} + a + b\right) \cdot L_{pile} + a \cdot b} \cdot \left(1 - \frac{x}{L_{pile}}\right) \quad (0 \leq x \leq L_{pile}) \tag{10}$$

Just like in the method of SSPM the displacement from each pile-group resulting in a vector, by using vector addition we can calculate the vector sum, se Appendix 7.

The Figure below shows the resultant vector direction from the two methods in relation to the bridge direction. The direction of the two vectors differs and the reason is that Hellman/Rehnman use the dimension of the whole pile group instead of the dimension of the combined piles. In this case a further vector addition should be done to get the exactly direction (i.e direction of the bridge). This will slightly decrease the magnitude of the displacement.

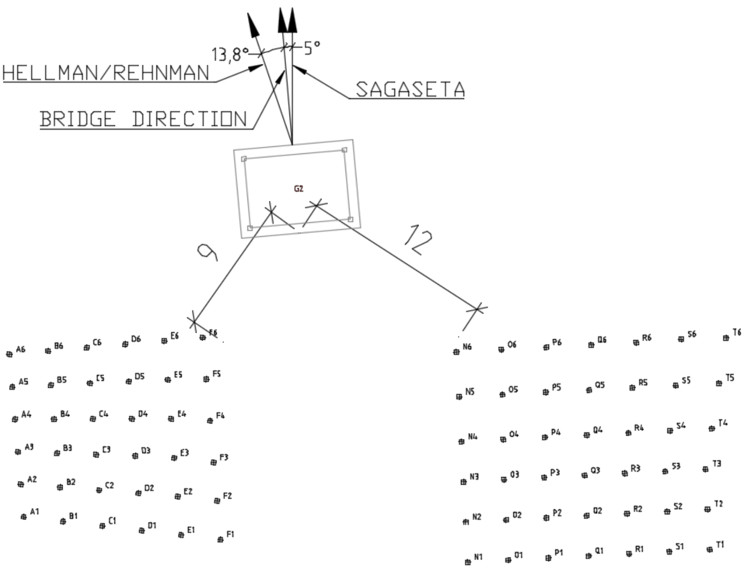

Figure 26. Resultants for analytical methods

4 RESULTS

4.1 Analytical calculations

Figure 27 shows a comparison between single pile calculation and the superposition technique. The result show that the superposition technique slightly overestimates the displacement compared to single pile calculation. The margin of error using the superposition technique containing 42 piles is 4% and increases with the amount of piles.

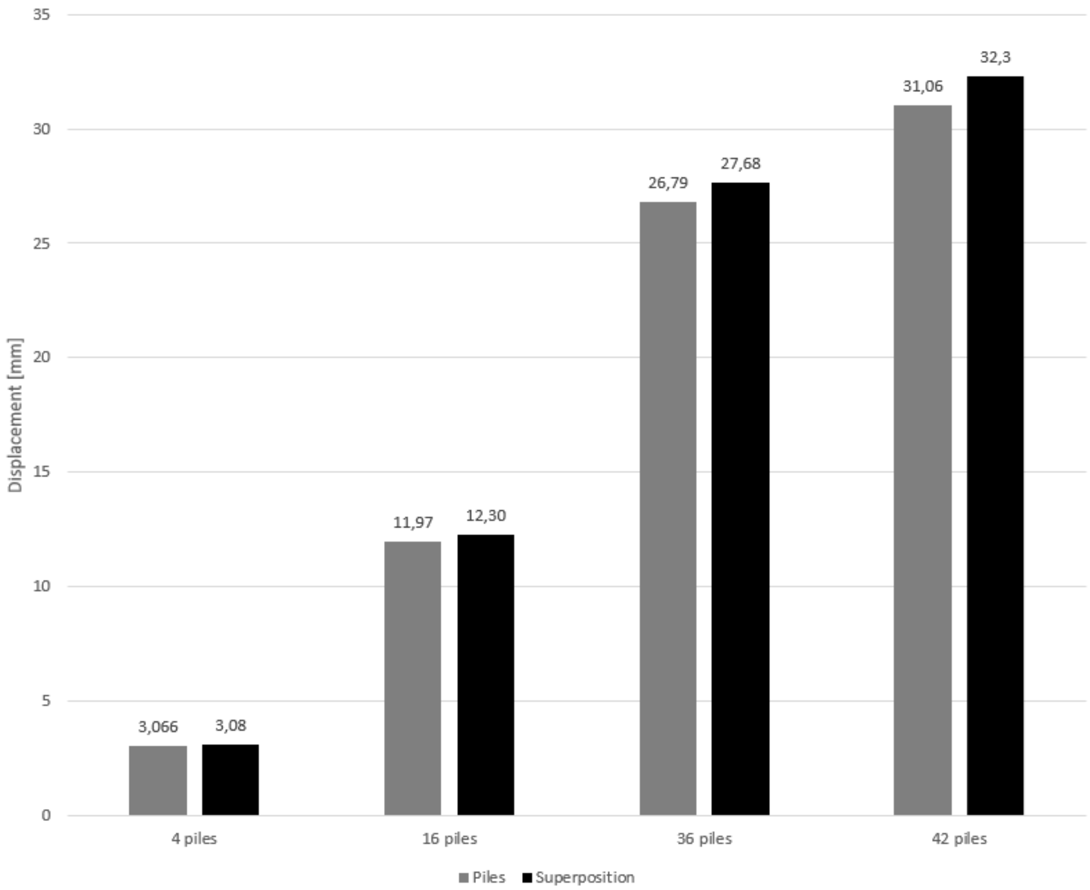

Figure 27. Comparison between single pile calculation and superposition

Table 3 shows the calculated displacement at surface for the methods of SSPM and Hellman/Rehnman.

Table 3. Displacement at surface

Displacement [mm]	Pre-boring excluded	Pre-boring included
SSPM	34.0	21.9
Hellman/Rehnman	32.6	28.1

In Figure 28 the result from the numerical calculation is presented and shows the horizontal displacement below surface.

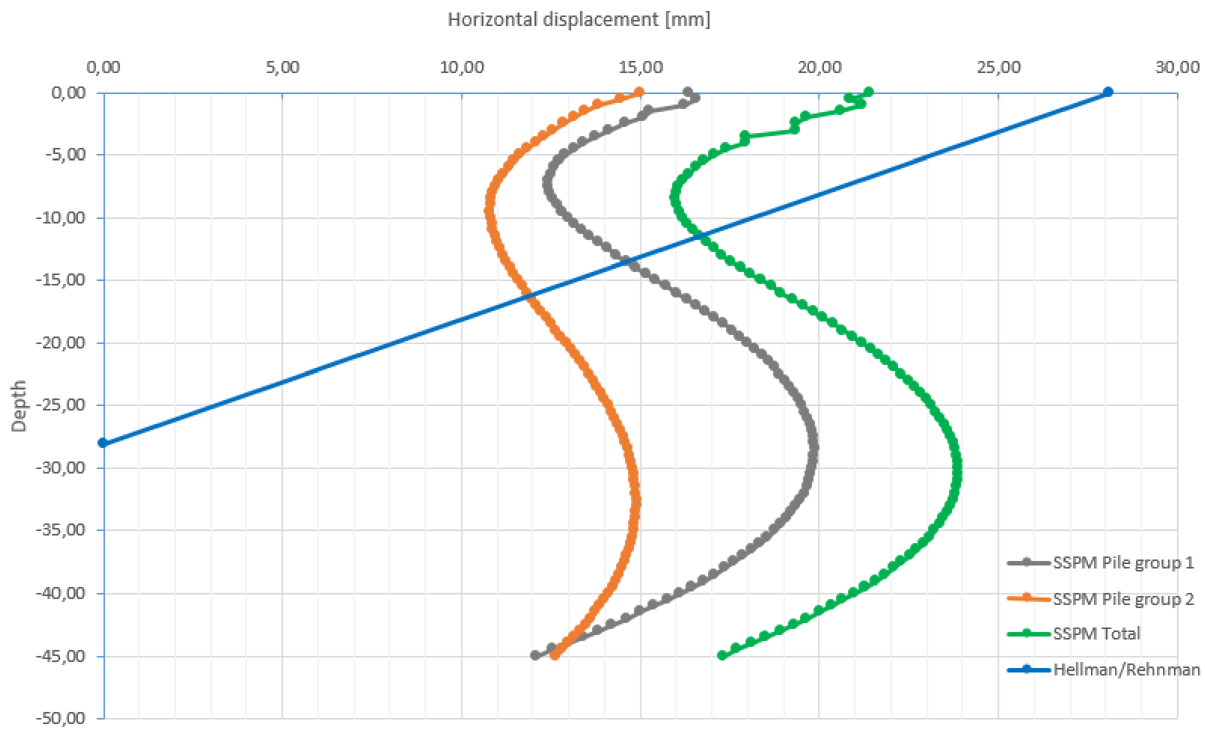

Figure 28. Horizontal displacement below surface

4.1.1 Discussion

The results when comparing superposition technique fulfils the theory regarding that the volume of the combined piles is equal to the displaced mass. However, it's important to understand that the margin of error will increase with a smaller distance from the pile group.

The results differs between the method of SSPM and Helman/Rehnman because there is fundamental differences between these two calculation methods. The first is the input geometry, Hellman/Rehnman uses the dimension of the whole pile group while SSPM use the dimension of the combined piles. The second difference is when looking at displacement below the surface. Hellman/Rehnman use a linear soil movement from studied point, while SSPM use numerical integration, hence the nonlinear result.

4.2 PLAXIS

Figure 29 is the result from the plane strain model and shows the movement pattern around a foundation. Figure 30 is the result from the axisymmetric model and shows the horizontal soil displacement below surface.

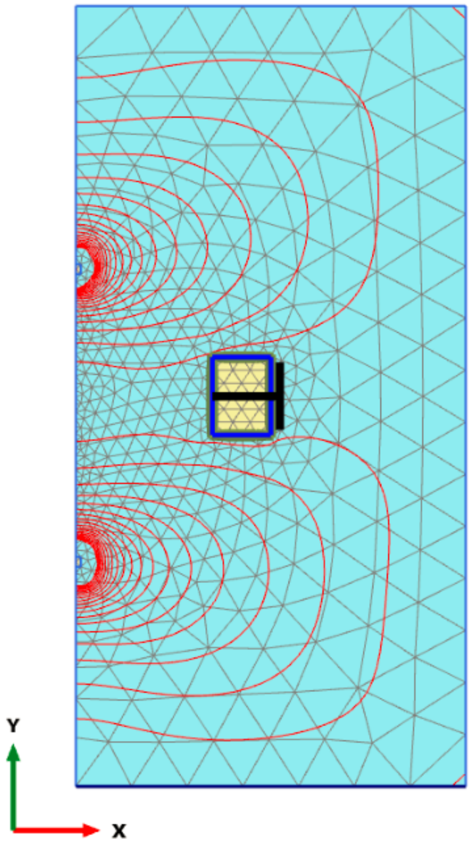

Figure 29. Soil movement around foundation

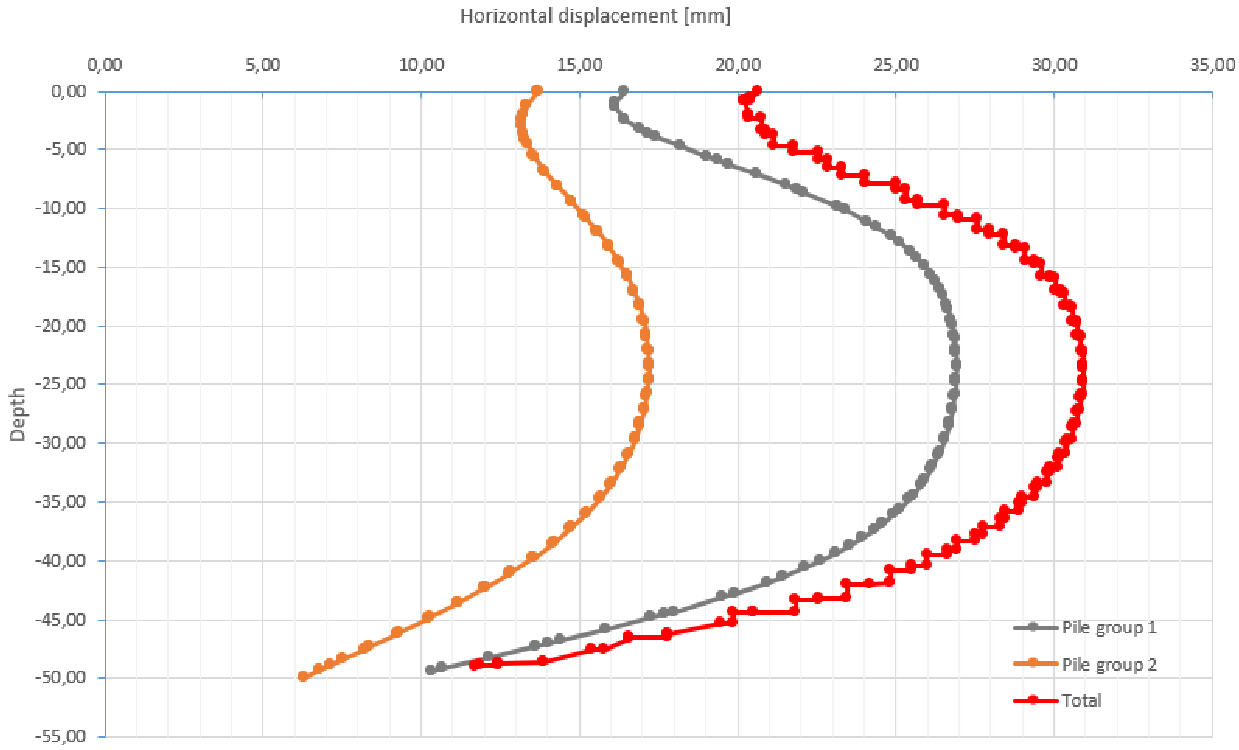

Figure 30. Soil displacement from PLAXIS axisymmetric model

4.2.1 Discussion

The VTE method in plane strain model is inadequate because it only take into account one horizontal plane (plan view) and all the displacement generated by the expansion is forced to move along this plane (i.e all displacement generated are forced to move horizontally). In reality the displacement generated by the expansion will displace between different levels, meaning that the soil will have an inclined movement upwards and therefore VTE method will result in an overestimation of the horizontal displacement. VTE method will be accurate close to the pile (where most of the displacement are lateral), but less accurate further from the pile. However, movement pattern and possible pore pressure at different depths can be evaluated from this method. Figure 29 also shows that the soil displacement are equalized between the two expansions, since it's a plan view the displacement can't move upwards as mentioned above, so there is no ability for the soil to heave.

The CEM in axisymmetric model is more suitable to calculate the displacement. This method allow the displacement to move between the levels in both horizontal and vertical direction. The possibility to model pre-boring is more preferable since we can change the expansion for the upper part of the pile.

4.3 Comparison

Figure 31 displays the combined result from each chapter above.

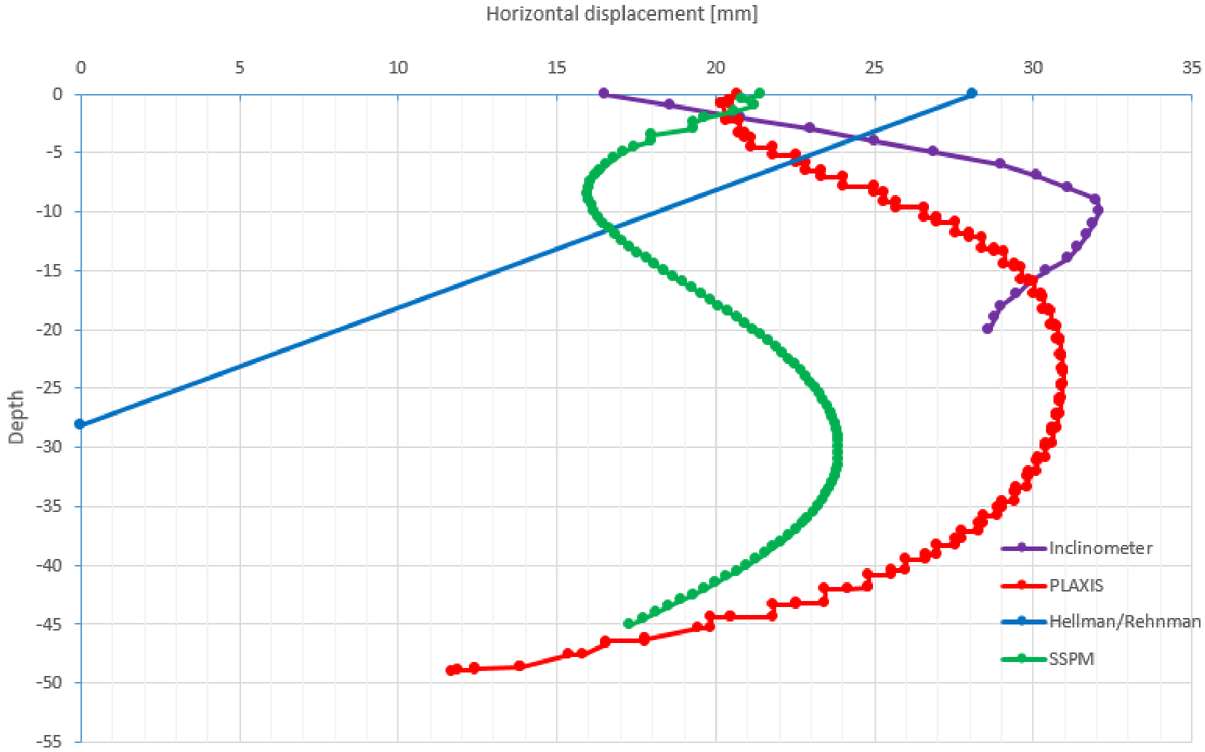

Figure 31. Comparison of soil displacement

4.3.1 Discussion

The measurement shows the lowest displacement at surface while it highly increase by depth. The comparison shows good agreement at surface between PLAXIS and SSPM. However, Hellman/Rehnman shows larger displacement. The reason that the measurement result is smaller should be the resisting force which none of the above methods takes into account. The resisting force could appear in two places; At the connection between bridge-foundation and at the pile foundation. However, since the measurement shows that the movement in the higher and lower prism are close to equal we can assume that the resisting force in the connection between bridge-foundation is negligible. Therefore we can assume that the resisting force occur in the pile foundation. The demands stated in the literature study regarding inclinometer measurement is not fulfilled, there have also been excavations close to the inclinometer pipes which most certainly have affected the accuracy.

5 CONCLUSION

The result shows that PLAXIS 2D axisymmetric model correlates best with the measured values on- and below surface. All the methods overestimates the displacement, this can be explained by the resisting force occurring in the foundation. Since the bridge connection is free to move in the displacement path the resisting force comprises by the existing pile foundation in investigated foundation G2.

Sagaseta's SSPM for single pile correlates well with PLAXIS result regarding surface displacement. When looking below surface the SSPM resulting in less displacement compared to PLAXIS 2D and field measurements, especially at a depth to 10 meters below surface. Hellman/Rehnman is the most inaccurate of the investigated methods and overestimating the surface displacement. Below surface it's useless since it only give a linear displacement from the investigated point which is uncorrelated from reality.

The result proves that the superposition technique can be used when calculating displacement. However, closer to the pile group the inaccuracy will increase and the displacement will be overestimated.

6 FURTHER RESEARCH

For further research it's would be preferable to have inclinometer measurements in the piles. With this data it would be possible to compare the displacement between the pile and the free soil surrounding it and to calculate the resisting force for the pile foundation. It's also recommended that the reference point for the inclinometer pipe would be fixed in something else than the investigated foundation, this to avoid the resisting force to affect the displacement for the free soil. A better solution could be to design a small concrete slab, lay it on the surface and fix the reference point. The surface displacement will continuously be measured with prisms and added to the displacement.

It should further be investigated the reliability of the superposition technique when studying at closer distance. In this paper only one foundation is investigated, due to the limited field measurements. It's recommended that more foundations is evaluated to get more reliable comparisons. It would be interesting to investigate a fixed bridge-foundation connection to see how much resisting force it will generate compare to our case.

7 REFERENCES

Bjerrum, L. (1963). Discussion to European Conf. on Soil Mech. and Found., (p. vol. 2). Weisbaden.

Bozozuk, M., Fellenius, B., & Samson, L. (1978). Soil disturbance from pile driving in sensitive clay. *Canadian Geotechnical Journal*, 346-361.

Butterfield, R., & Bannerjee, P. (1970). The Effect of Porewater Pressures on the Ultimate Bearing Capacity of Driven Piles. *The Second Southeast Asian Conference on Soil Engineering* (pp. 385-394). Singapore: Souteast Asian Geotechnical Society.

Dijkstra, J. (2015). *On displacement pile installation in sand and clay.* Gothenburg: Chalmers University of Technology.

Dijkstra, J., Ottolini, M., & van Tol, F. (2014). *Immediate and long-term installation effects adjacent to an open-ended pile in a layered clay.* Gothenburg: Chalmers University of Technology.

Edstam, T. (2012). *Skäransbrons rörelser vid pålslagning för den närliggande Partihallsbron.* Göteborg: Skanska Sverige AB.

Geodestek. (2009, 02 02). *Digital Vertical Inclinometer System.* Retrieved from Geodestek: http://www.geodestek.com/Docs/Digital_Vertical_Inclinometer_System.pdf

Hellman, L. (1981). *Om grundläggningsteknik i tätort.* Byggnadskonst, Vol. 73, No. 10.

Hintze, S., Liedberg, S., Massarsch, R., Hanson, M., Lundahl, B., & Rehnman, S.-E. (1997). *Omgivningspåverkan vid pål- och spontslagning.* Linköping: Comission on Pile Research.

Knappett, J. A., & Craig, R. F. (2012). *Craig's Soil Mechanics.* Abingdon: Spon Press.

Larsson, R. (2008). *Jords egenskaper.* Linköping: Swedish Geotechnical Institute.

Lehane, B., & D. G. (2004). *Displacement fields induced by penetrometer installation in an artificial soil.* International Journal of Physical Modelling in Geotechnics.

Lehane, B., & Jardine, R. (1993). *Displacement-pile behaviour in a soft marine clay.* London: Imperial College.

Leica-Geosystems. (2013, 05 10). *Leica-geosystems.* Retrieved from Leica TS30/TM30 User Manual: http://surveyequipment.com/assets/index/download/id/220/

Massarsch, K. R., & Wersäll, C. (2013). *Cumulative Lateral Soil Displacement Due to Pile Driving in Soft Clay.* Stockholm: Royal Institute of Technology.

Ni, Q., Hird, C., & Guymer, I. (2010). *Physical modelling of pile penetration in clay using transparent soil and particle image velocimetry.* Géotechnique 60.

Olsson, C., & Holm, G. (1993). *Pålgrundläggning.* Linköping: Statens geotekniska institut.

Potts, D., & Zdravkovic´, L. (2001). *Finit element analysis in geotechnical engineering.* London: Thomas Telford.

Sagaseta, C. (1987). Analysis of undrained soil deformation due to ground loss. *Geotechnique 37*, 301-320.

Sagaseta, C. (1997). Deformation analysis of shallow penetration in clay. *International Journal for Numerical and Analytical Methods in Geomechanics*, 687-719.

Sheil, B., McCabe, B., Hunt, C., & Pestana, J. (2015). *A practical approach for the consideration of single pile and pile group installation effects in clay: Numerical modelling.* Galway: Journal of Geo-Engineering Sciences.

Skempton, A., & Macdonald, D. (1956). *The Allowable Settlement of Buildings.* London: Proc. I.C.E.

Stark, T., & Choi, H. (2007). *Slope inclinometers for landslides.* Urbana: University of Illinois at Urbana-Champaign.

Whittle, A., & Sagaseta, C. (2001). Predictions of Ground Movements due to Pile Driving in Clay. *Journal of Geotechnical and Geoenvironmental engineering, ASCE*, 55-56.

8 APPENDICES

Appendix 1. Pictures from test site

Figure 32. Prism for measuring vertical- and horizontal movements

Figure 33. Inclinometer for measuring soil displacement

Figure 34. Inclinometer for measuring pile displacement

Figure 35. Total station for reading of the prism's

Appendix 2. Pile groups 1 & 2

Table 4. Pile group 1

Pilegroup 1				Preboring	Effective
7902-423BNVA				(1=YES)	length (m)
A1	215	SP2	2014-07-01	1	51
B1	215	SP2	2014-06-30	0	51
C1	215	SP2	2014-06-27	1	51
D1	215	SP2	2014-06-26	0	51
E1	215	SP2	2014-06-26	1	51
F1	215	SP2	2014-06-25	1	51
F2	215	SP2	2014-06-25	0	51
E2	215	SP2	2014-06-26	1	51
D2	215	SP2	2014-06-27	1	51
C2	215	SP2	2014-06-30	0	51
B2	215	SP2	2014-06-30	1	51
A2	215	SP2	2014-07-01	0	51
A3	215	SP2	2014-07-01	1	45
B3	215	SP2	2014-06-30	0	45
C3	215	SP2	2014-06-30	1	45
D3	215	SP2	2014-06-27	0	45
E3	215	SP2	2014-06-26	1	45
F3	215	SP2	2014-06-25	0	45
F4	215	SP2	2014-06-25	0	45
E4	215	SP2	2014-06-26	1	45
D4	215	SP2	2014-06-27	1	45
C4	215	SP2	2014-06-30	0	45
B4	215	SP2	2014-06-30	1	45
A4	215	SP2	2014-06-30	0	45
A5	215	SP2	2014-06-30	1	39
B5	215	SP2	2014-07-01	0	39
C5	215	SP2	2014-07-01	1	39
D5	215	SP2	2014-06-27	0	39
E5	215	SP2	2014-06-26	0	39
F5	215	SP2	2014-06-25	1	39
F6	215	SP2	2014-06-26	1	39
E6	215	SP2	2014-06-26	1	39
D6	215	SP2	2014-06-27	1	39
C6	215	SP2	2014-07-01	0	39
B6	215	SP2	2014-07-01	1	39
A6	215	SP2	2014-07-01	0	39
				20	45

Table 5. Pile group 2

Pile group 2			Preboring	Effective
7902-423BNOD			(1=JA)	längd (m)

N1	215	SP2	2014-06-16	1	65
O1	215	SP2	2014-06-17	1	65
P1	215	SP2	2014-06-18	1	65
Q1	215	SP2	2014-06-18	0	65
R1	215	SP2	2014-06-19	1	65
S1	215	SP2	2014-06-19	0	65
T1	215	SP2	2014-06-19	1	65
T2	215	SP2	2014-06-23	0	56
S2	215	SP2	2014-06-23	1	56
R2	215	SP2	2014-06-23	0	56
Q2	215	SP2	2014-06-23	1	56
P2	215	SP2	2014-06-18	0	56
O2	215	SP2	2014-06-17	1	56
N2	215	SP2	2014-06-16	1	56
N3	215	SP2	2014-06-16	1	56
O3	215	SP2	2014-06-17	1	56
P3	215	SP2	2014-06-18	1	56
Q3	215	SP2	2014-06-23	0	56
R3	215	SP2	2014-06-23	1	56
S3	215	SP2	2014-06-23	0	56
T3	215	SP2	2014-06-23	1	56
T4	215	SP2	2014-06-24	0	47
S4	215	SP2	2014-06-24	1	47
R4	215	SP2	2014-06-24	0	47
Q4	215	SP2	2014-06-24	1	47
P4	215	SP2	2014-06-18	0	47
O4	215	SP2	2014-06-17	1	47
N4	215	SP2	2014-06-17	1	47
N5	215	SP2	2014-06-17	1	47
O5	215	SP2	2014-06-18	1	47
P5	215	SP2	2014-06-18	1	47
Q5	215	SP2	2014-06-24	0	47
R5	215	SP2	2014-06-24	1	47
S5	215	SP2	2014-06-24	0	47
T5	215	SP2	2014-06-24	1	47
T6	215	SP2	2014-06-24	0	39
S6	215	SP2	2014-06-24	1	39
R6	215	SP2	2014-06-24	0	39
Q6	215	SP2	2014-06-24	1	39
P6	215	SP2	2014-06-18	0	39
O6	215	SP2	2014-06-18	1	39
N6	215	SP2	2014-06-17	1	39
				27	52

Appendix 3. Profile and plan drawings

Profile view over the pile area

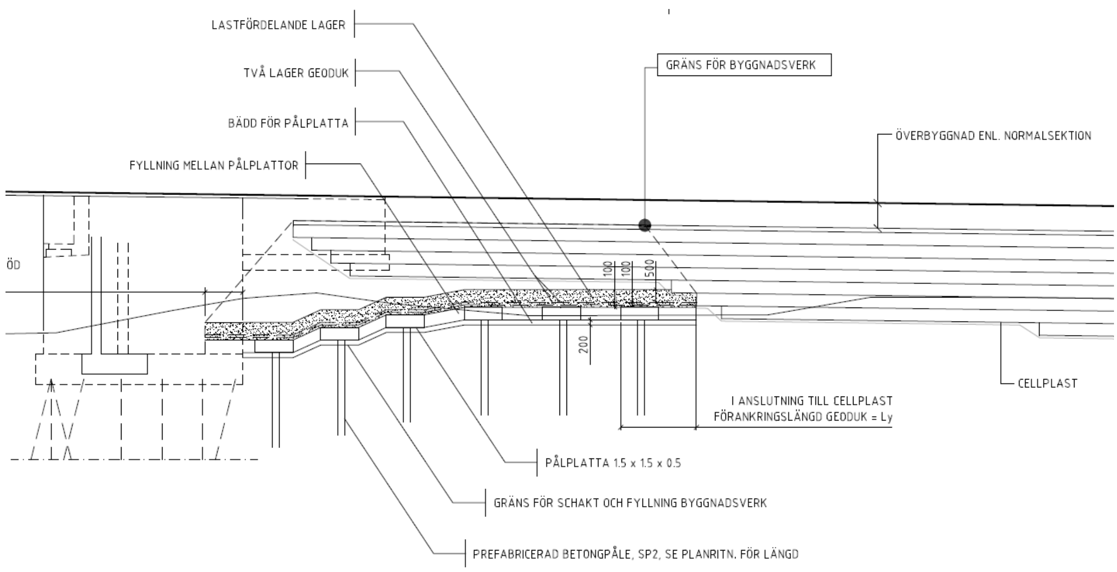

Plan view, pile area D

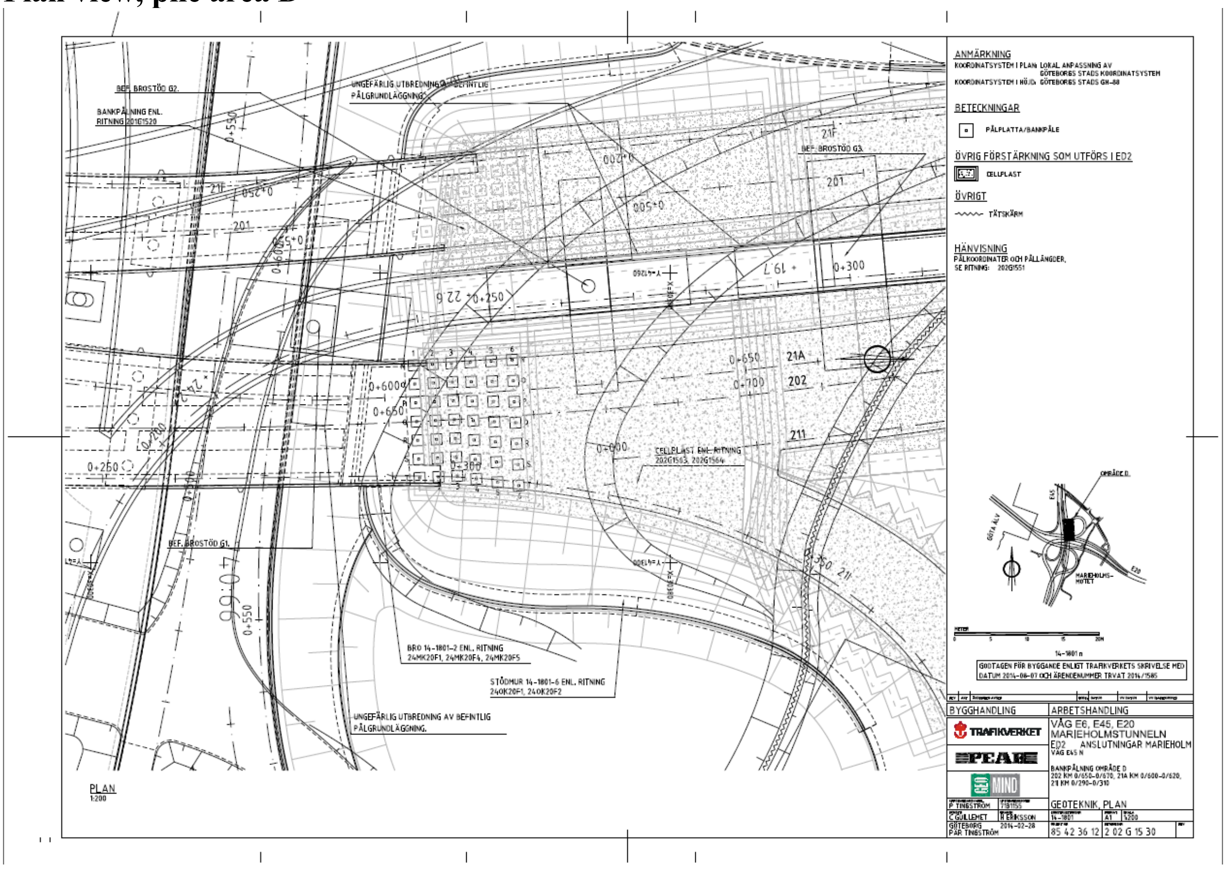

Plan view, pile area A

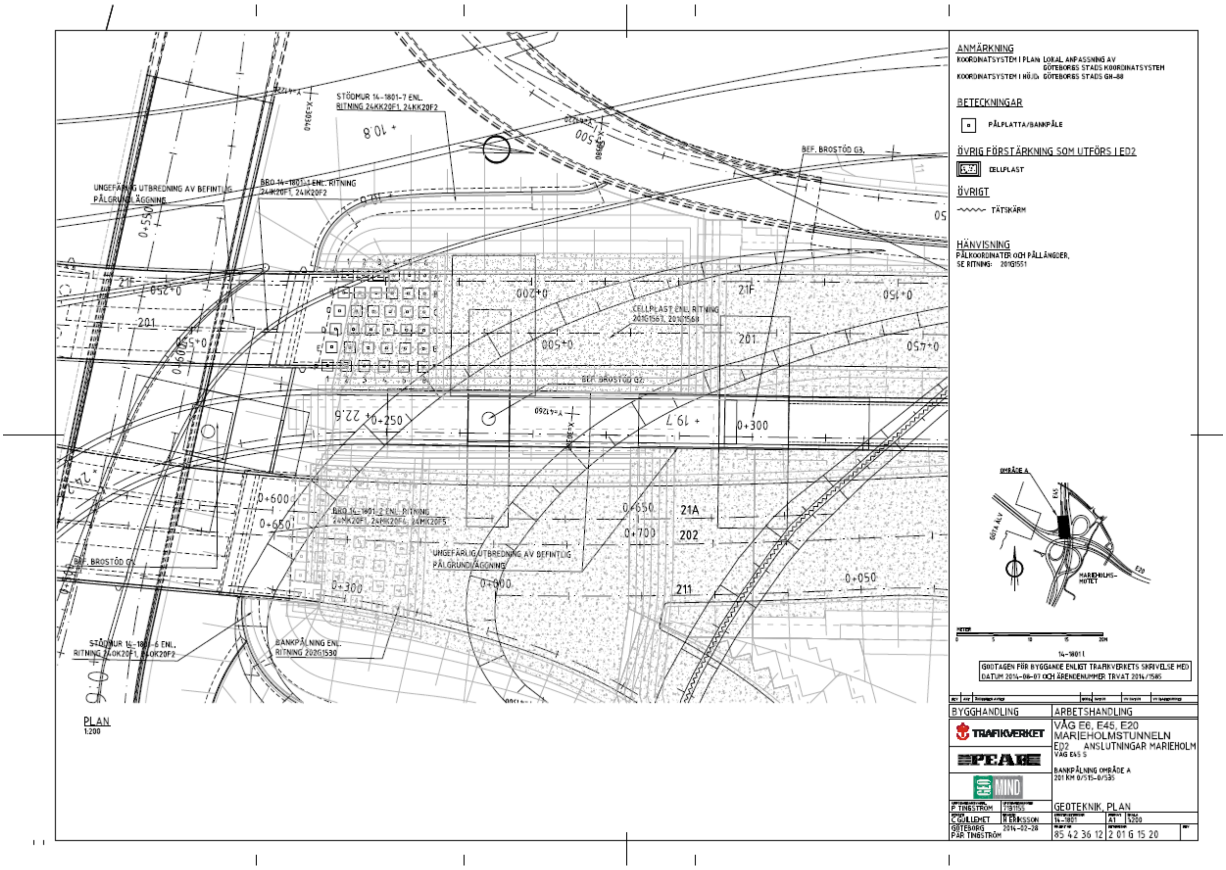
ANMÄRKNING
KOORDINATSYSTEM I PLAN: LOKAL ANPASSNING AV GÖTEBORGS STADS KOORDINATSYSTEM
KOORDINATSYSTEM I HÖJD: GÖTEBORGS STADS GH-88
BETECKNINGAR
PÅLPLATTA/BANKPÅLE
ÖVRIG FÖRSTÄRKNING SOM UTFÖRS I ED2
CELLPLAST
ÖVRIGT
TÄTSKÄRM
HÄNVISNING
PÅLKOORDINATER OCH PÅLLÄNGDER, SE RITNING: 201G1551
MARIEHOLMS-MOTET
E20
14-1801 L
GODTAGEN FÖR BYGGANDE ENLIGT TRAFIKVERKETS SKRIVELSE MED DATUM 2014-06-07 OCH ÄRENDENUMMER TRVAT 2014/1585
BYGGHANDLING
ARBETSHANDLING
VÄG E6, E45, E20
MARIEHOLMSTUNNELN
ED2 ANSLUTNINGAR MARIEHOLM
VÄG E45 S
BANKPÅLNING OMRÅDE A
201 KM 0/515-0/535
GEOTEKNIK, PLAN
P TINGSTRÖM
C GUILLEMET
H ERIKSSON
14-1801
A1
1:200
GÖTEBORG
PÄR TINGSTRÖM
2014-02-28
85 42 36 12
2 01 G 15 20
PLAN
1:200
STÖDMUR 14-1801-7 ENL. RITNING 24KK20F1, 24KK20F2
BEF. BROSTÖD G3
BEF. BROSTÖD G2
BEF. BROSTÖD G1
CELLPLAST ENL. RITNING 201G1567, 201G1568
BANKPÅLNING ENL. RITNING 202G1530
UNGEFÄRLIG UTBREDNING AV BEFINTLIG PÅLGRUNDLÄGGNING

Appendix 4. Validation of superposition technique

Table 6. Comparison, n=4 piles

Pile	r	Direction	Displacement	Vector addition
20	13,7	95,9	0,85	
21	13,7	84,1	0,85	
28	16,5	94,9	0,69	
29	16,5	85,1	0,69	
				3,066

Superpile	
N	4,000
L	50,000
A	0,303
R	0,310
r	15
	3,08

Table 7. Comparison, n=16 piles

Pile	r	Direction	Displacement	Vector addition
11	11,6	111,3	1,0113	
12	10,9	97,4	1,0794	
13	10,9	82,6	1,0794	
14	11,6	68,7	1,0113	
19	14,2	107,2	0,8158	
20	13,7	95,9	0,8477	
21	13,7	84,1	0,8477	
22	14,2	72,8	0,8158	
27	16,9	104,4	0,6750	
28	16,5	94,9	0,6931	
29	16,5	85,1	0,6931	
30	16,9	75,6	0,6750	
35	19,6	102,3	0,5720	
36	19,3	94,2	0,5821	
37	19,3	85,8	0,5821	
38	19,6	77,7	0,5720	
				11,97

Superpile	
N	4,000
L	50,000
A	1,210
R	0,621
r	15
	12,30

Table 8. Comparison, n=36 piles

Pile	r	Direction	Displacement	Vector addition
2	10,6	131,2	1,11	
3	9	117,7	1,32	

4	8,1	99,9	1,47	
5	8,1	80,1	1,47	
6	9	62,3	1,32	
7	10,6	48,8	1,11	
10	12,9	123	0,90	
11	11,6	111,3	1,01	
12	10,9	97,4	1,08	
13	10,9	82,6	1,08	
14	11,6	68,7	1,01	
15	12,9	57	0,90	
18	15,3	117,2	0,75	
19	14,2	107,2	0,82	
20	13,7	95,9	0,85	
21	13,7	84,1	0,85	
22	14,2	72,8	0,82	
23	15,3	62,8	0,75	
26	17,8	113,1	0,64	
27	16,9	104,4	0,68	
28	16,5	94,9	0,69	
29	16,5	85,1	0,69	
30	16,9	75,6	0,68	
31	17,8	66,9	0,64	
34	20,4	110	0,55	
35	19,6	102,3	0,57	
36	19,3	94,2	0,58	
37	19,3	85,8	0,58	
38	19,6	77,7	0,57	
39	20,4	70	0,55	
42	23,1	107,7	0,47	
43	22,4	100,8	0,49	
44	22	93,6	0,50	
45	22	86,4	0,50	
46	22,4	79,2	0,49	
47	23,1	72,3	0,47	
				26,79

Superpile	
N	4,000
L	50,000
A	2,723
R	0,931
r	15
	27,68

Appendix 5. Soil properties and model parameters

Table 9. Soil properties

Level [m]	W_L [%]	Weight [kN/m^3]	σ'_c [kPa]	c_u [kPa]		E'_{50} [kPa]
10	75	15,3	40	14		4250
5	78	15,7	62	22		4875
0	75	15,8	90	30		5500
-10	75	16	140	47		6750
-15	71	16,5	189	60		7375
-20	68	16,5	235	72		8625
-25	68	16,5	280	86		9250
-30	70	16	308	97		9875
-40	73	16,5	360	118		11125
-60	73	17	482	158		13625

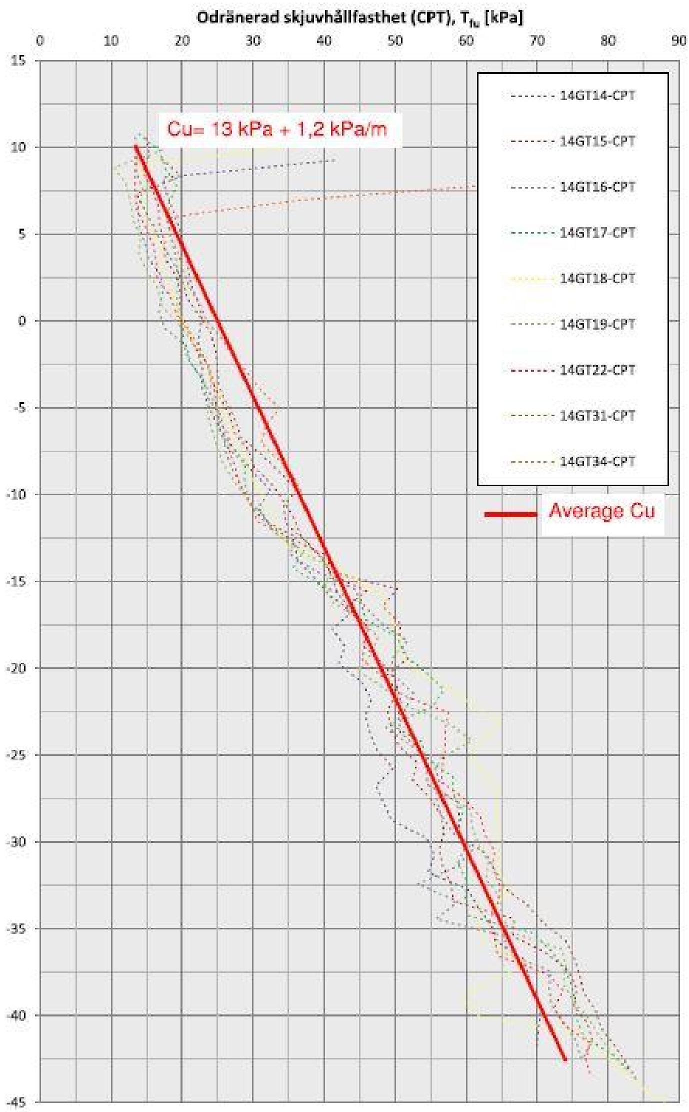

Figure 36. CPT test

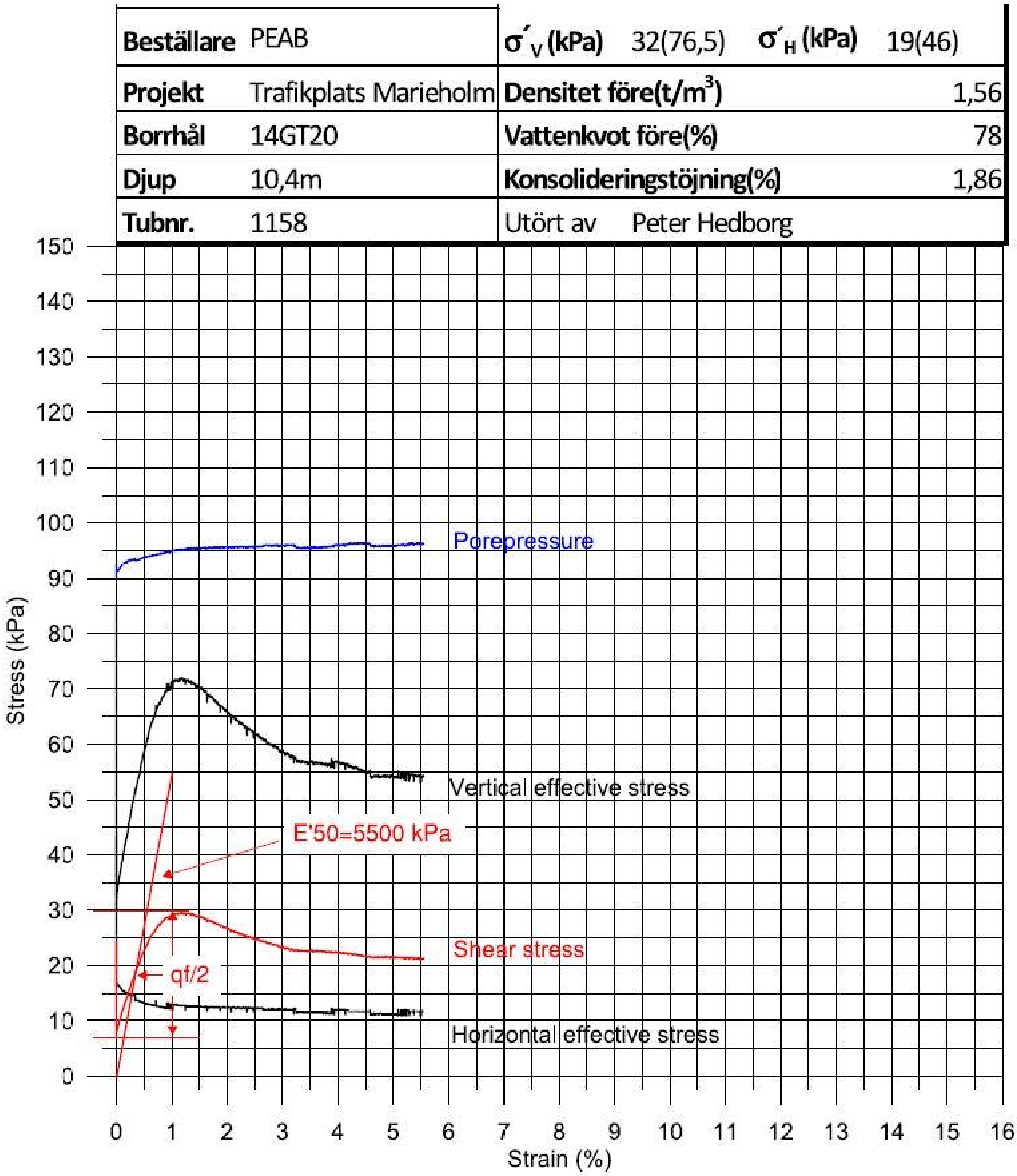

Figure 37. Triaxial test at 10 m

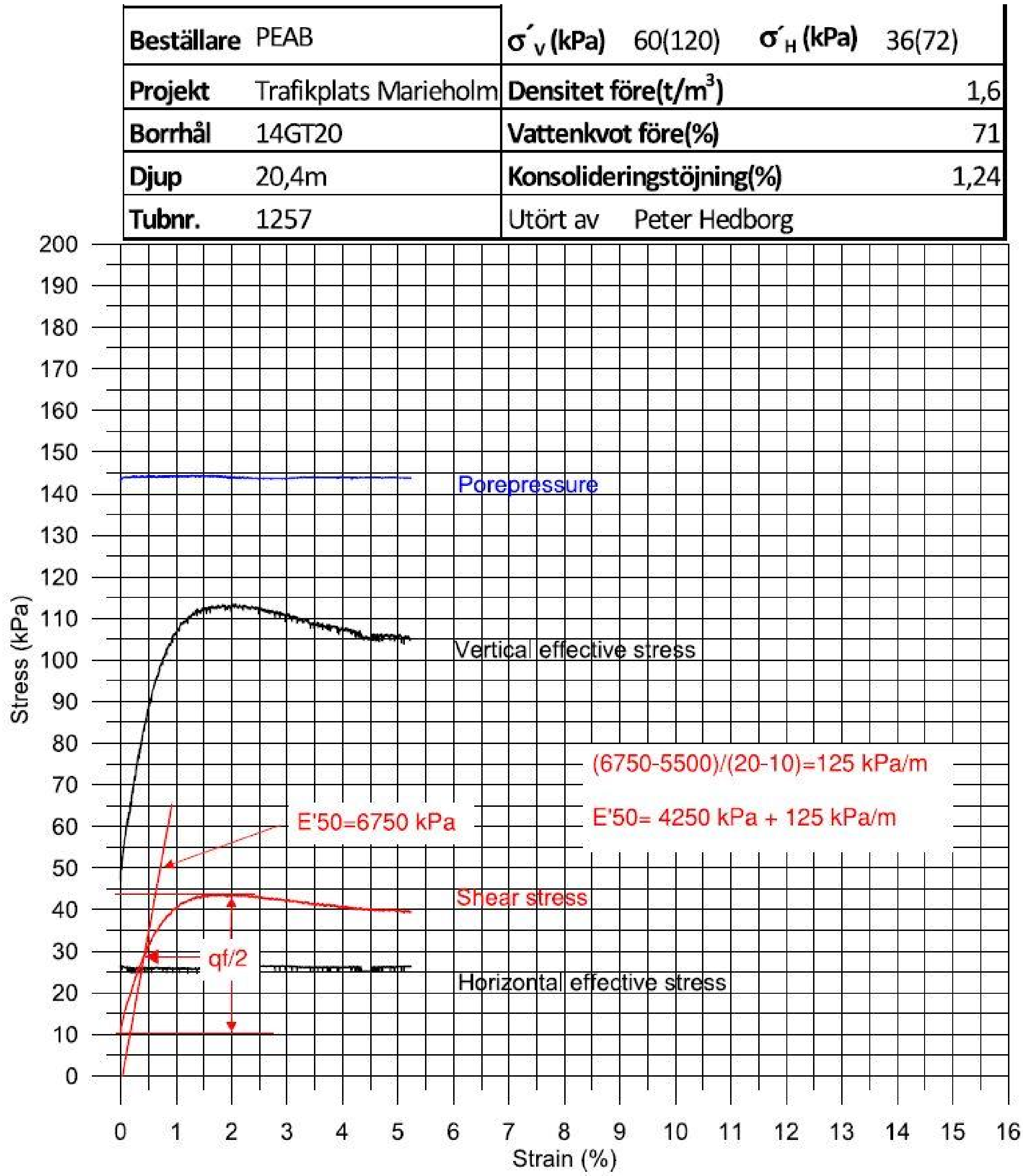

Figure 38. Triaxial test at 20 m

Appendix 6. SSPM

Table below shows the input and results when calculating the displacement at surface.

	Pile group 1		
N [st]	36		
Lpile [m]	45		
Lpreboring [m]	12		
	Super pile 1	**Pre-boring 1**	
N [st]	36	20	
Acircel [m2]	0,0756	0,0756	
Asuperpile [m2]	2,7225	1,5125	
Rsuperpile [m]	0,9311	0,69403739	
r, distance [m]	15	15	
δr [m]	0,02735	-0,01003	
Σδr	0,01732		
	Pile group 2		
N [st]	42		
Lpile [m]	52		
Lpreboring [m]	12		
	Super pile 2	**Pre-boring 2**	
N [st]	42	27	
Acircle [m2]	0,0756	0,0756	
Asuperpile [m2]	3,1763	2,041875	
Rsuperpile [m]	1,0058	0,806398575	
r, distance [m]	21	21	
δr [m]	0,02234	-0,00767	
Σδr	0,01467		
	Pre-boring excl.	**Pre-boring inc.**	
Σδr,tot [mm]	49,69	31,99	
Σδr,tot,corrected [mm]	34	21,9	corrected with vector addition at 90 deg

Below the numerical calculations regarding displacement below surface is presented.

R = Pile radius

r = radial distance

z = vertical distance

h = embedment depth

STEP 1 - Point source at S(0,h):

$$v_{r1}(R,r,z,h) := \frac{R^2 r}{4\cdot\left(r_1(r,z,h)\right)^3}$$

$$r_1(r,z,h) := \sqrt{r^2 + (z-h)^2}$$

STEP 2 - Image point sink at S'(0,-h):

$$v_{r2}(R,r,z,h) := \frac{-\left(R^2\right)r}{4\cdot\left(r_2(r,z,h)\right)^3}$$

$$r_2(r,z,h) := \sqrt{r^2 + (z+h)^2}$$

STEP 3 - Corrective surface shear tractions:

$$v_{r3}(R,r,z,h) := \int_0^{100\cdot R} I_r(r,z,a)\cdot F_{\gamma SP}(R,h,a)\,da$$

$$F_{\gamma SP}(R,h,a) := 3\cdot R^2\cdot\frac{h\cdot a}{r_h(a,h)^5}$$

$$r_h(a,h) := \sqrt{a^2 + h^2}$$

$$I_r(r,z,a) := \frac{1}{2\cdot\pi}\cdot\left(A_{rK}(r,a,z)\cdot K(r,a,z) + A_{rE}(r,a,z)\cdot E(r,a,z)\right)$$

$$A_{rK}(r,a,z) := \frac{r_{a2}(r,a,z)}{r}\cdot\left[1 - \frac{2\cdot a\cdot r - z^2}{\left(r_{a2}(r,a,z)\right)^2}\right]$$

$$r_{a1}(r,a,z) := \sqrt{(a-r)^2 + z^2} \quad r_{a2}(r,a,z) := \sqrt{(a+r)^2 + z^2}$$

$$K(r,a,z) := \int_0^{\frac{\pi}{2}} \frac{1}{\sqrt{1 - k(r,a,z)^2\cdot\sin(\theta)^2}}\,d\theta$$

$$k(r,a,z) := \sqrt{1 - \frac{r_{a1}(r,a,z)^2}{r_{a2}(r,a,z)^2}}$$

$$A_{rE}(r,a,z) := \frac{-r_{a2}(r,a,z)}{r}\cdot\left[1+\frac{z^2}{2}\cdot\left[\frac{1}{\left(r_{a1}(r,a,z)\right)^2}+\frac{1}{\left(r_{a2}(r,a,z)\right)^2}\right]\right]$$

$$E(r,a,z) := \int_0^{\frac{\pi}{2}} \sqrt{1-k(r,a,z)^2\cdot\sin(\theta)^2}\,d\theta$$

FINAL STEP:

$$\delta_r(R,h,z,r) := \int_0^h \left(v_{r1}(R,r,z,h)+v_{r2}(R,r,z,h)+v_{r3}(R,r,z,h)\right)dh$$

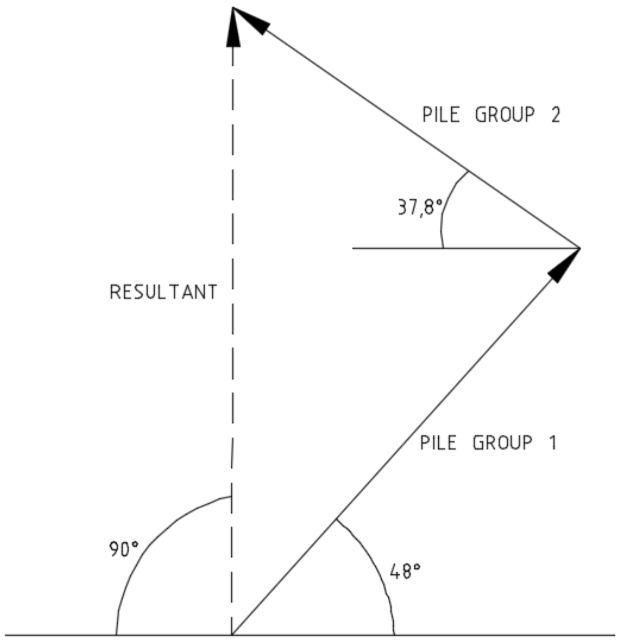

Appendix 7. Hellman/Rehnman

	Pile group 1	Pre-boring 1	
α [deg]	53,4	53,4	
L [m]	45	12	
x [m]	9	9	
a [m]	13,3	13,3	
b [m]	12,6	12,6	
ΣVpile [m3]	122,5	-18,2	
δr [m]	0,0243	-0,0068	
δr,tot1 [m]	0,0175		
	Pile group 2	**Pre-boring 2**	
α [deg]	33,1	-	
L [m]	52	-	
x [m]	12	-	
a [m]	17	-	
b [m]	14,3	-	
		-	
ΣVpile [m3]	164,1	-	
δr [m]	0,0231	-	
δr,tot2 [m]	0,0231		
	Pre-boring excl.	**Pre-boring inc.**	
δr,tot [mm]	47,4	40,6	
δr,tot,corrected [mm]	32,6	28,1	corrected with vector addition, resultant at 108,5 deg

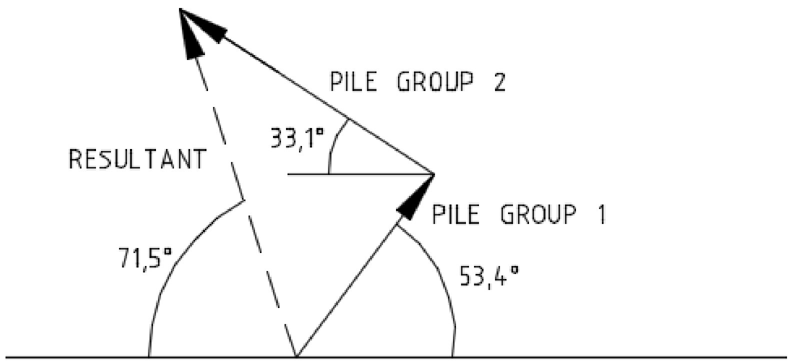

Appendix 8. PLAXIS, plane strain model

Figure 39 shows the soil movement from the plane strain model. The geometry is not matched for our specific case. Here we can see the formation of a wedge in front of the foundation.

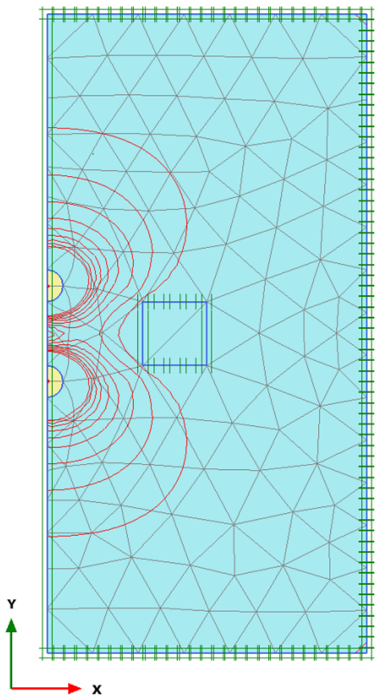

Figure 39. Cavity expansion

In Figure 40 the distance and geometry is matched for our specific case. At this distance the movement from the two super piles eliminates large part of the wedge. However the flow pattern is the same as in Figure 29.

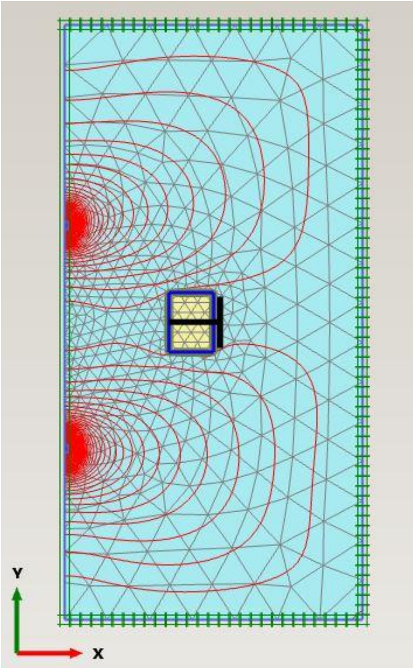

Figure 40. Soil movement around foundation

Figure 41 illustrate the soil displacement in a cross section. Here we can clearly see that the displacement decreases closer to the foundation.

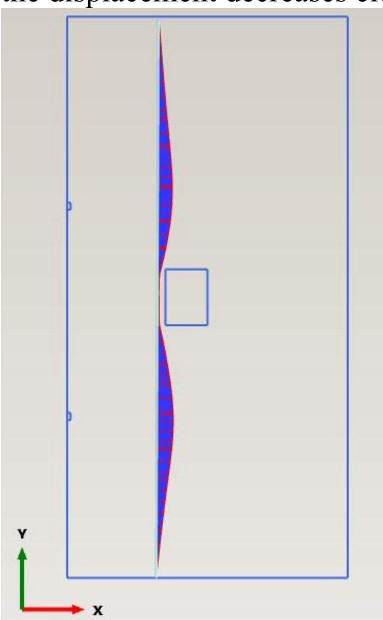

Figure 41. Horizontal displacement around foundation

Appendix 9. PLAXIS, Axisymmetric model

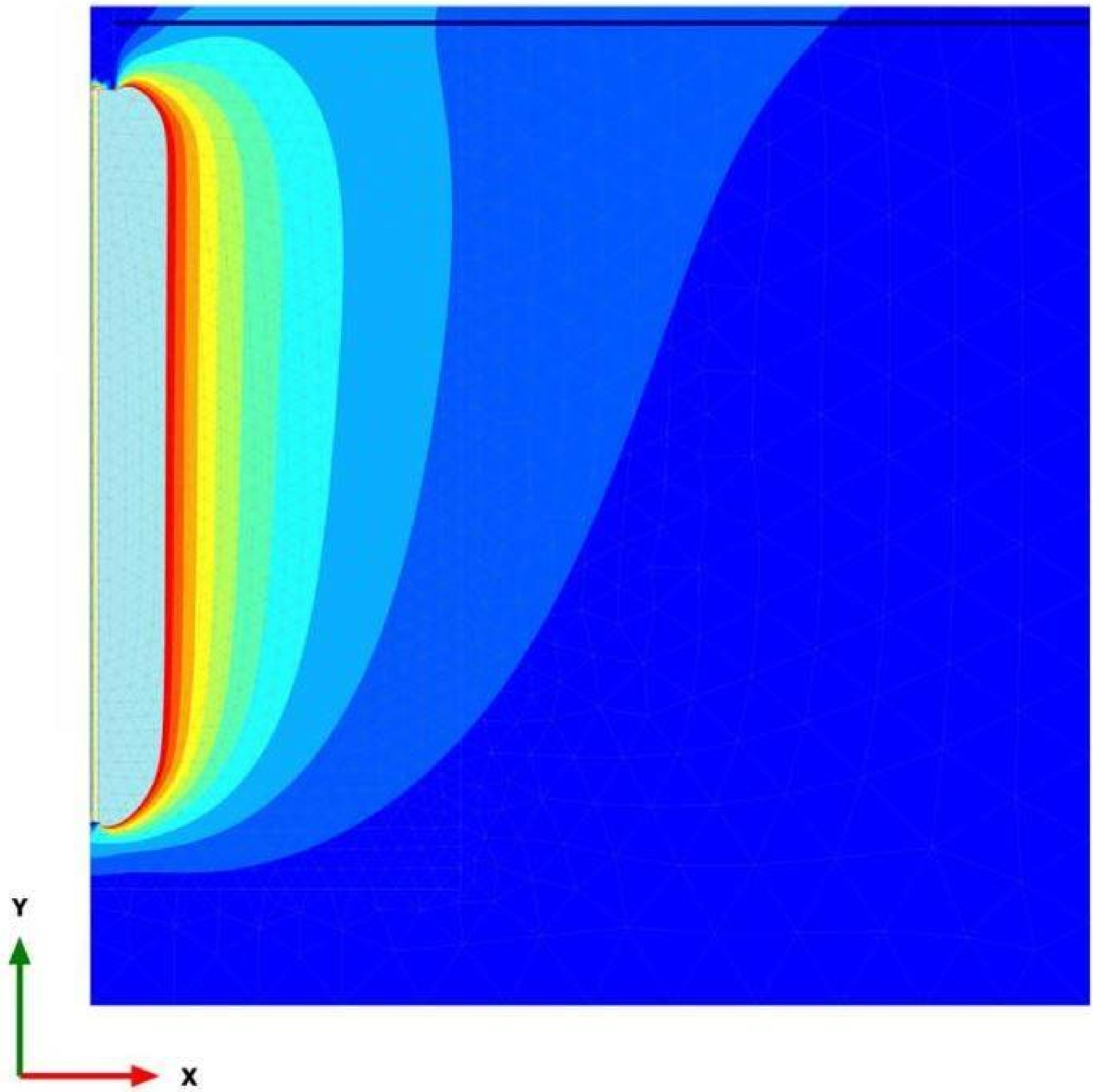

Figure 42. Output result

Table 10. Displacement

Horizontal displacement at 15m				Horizontal displacement at 21m				Total displacement	
Y [m]	Ux [m]	Ux [mm]		Y [m]	Ux [m]	Ux [mm]		Y	Ux
0,00	0,02	17,75		0,00	0,02	15,15		0,00	22,52
-1,01	0,02	17,46		-0,10	0,02	15,11		-0,62	22,28
-1,01	0,02	17,46		-0,10	0,02	15,11		-0,62	22,28
-1,19	0,02	17,46		-1,24	0,01	14,76		-0,84	22,06
-1,19	0,02	17,46		-1,24	0,01	14,76		-0,84	22,06
-1,39	0,02	17,47		-2,03	0,01	14,64		-0,89	22,00
-1,39	0,02	17,47		-2,03	0,01	14,64		-0,89	22,00
-2,38	0,02	17,77		-2,47	0,01	14,61		-2,08	22,20
-2,38	0,02	17,77		-2,47	0,01	14,61		-2,08	22,20
-3,28	0,02	18,31		-3,03	0,01	14,60		-2,34	22,61
-3,28	0,02	18,31		-3,03	0,01	14,60		-2,34	22,61
-3,57	0,02	18,52		-3,65	0,01	14,63		-3,35	22,79

-3,57	0,02	18,52		-3,65	0,01	14,63		-3,35	22,79
-3,88	0,02	18,77		-4,10	0,01	14,68		-3,78	23,00
-3,88	0,02	18,77		-4,10	0,01	14,68		-3,78	23,00
-4,75	0,02	19,53		-4,61	0,01	14,75		-4,62	23,64
-4,75	0,02	19,53		-4,61	0,01	14,75		-4,62	23,64
-5,59	0,02	20,33		-5,46	0,01	14,91		-5,19	24,36
-5,59	0,02	20,33		-5,46	0,01	14,91		-5,19	24,36
-5,93	0,02	20,66		-5,65	0,01	14,95		-5,88	24,65
-5,93	0,02	20,66		-5,65	0,01	14,95		-5,88	24,65
-6,27	0,02	21,00		-6,78	0,02	15,23		-6,56	25,06
-6,27	0,02	21,00		-6,78	0,02	15,23		-6,56	25,06
-7,11	0,02	21,81		-6,87	0,02	15,25		-7,14	25,73
-7,11	0,02	21,81		-6,87	0,02	15,25		-7,14	25,73
-8,05	0,02	22,66		-8,09	0,02	15,59		-7,92	26,59
-8,05	0,02	22,66		-8,09	0,02	15,59		-7,92	26,59
-8,42	0,02	22,98		-8,15	0,02	15,60		-8,40	26,86
-8,42	0,02	22,98		-8,15	0,02	15,60		-8,40	26,86
-8,64	0,02	23,16		-9,38	0,02	15,95		-9,25	27,19
-8,64	0,02	23,16		-9,38	0,02	15,95		-9,25	27,19
-9,83	0,02	24,06		-9,44	0,02	15,97		-9,66	27,93
-9,83	0,02	24,06		-9,44	0,02	15,97		-9,66	27,93
-10,16	0,03	24,28		-10,66	0,02	16,30		-10,58	28,28
-10,16	0,03	24,28		-10,66	0,02	16,30		-10,58	28,28
-11,13	0,03	24,86		-10,73	0,02	16,32		-10,92	28,77
-11,13	0,03	24,86		-10,73	0,02	16,32		-10,92	28,77
-11,55	0,03	25,08		-11,94	0,02	16,61		-11,89	29,10
-11,55	0,03	25,08		-11,94	0,02	16,61		-11,89	29,10
-12,42	0,03	25,48		-12,01	0,02	16,63		-12,18	29,44
-12,42	0,03	25,48		-12,01	0,02	16,63		-12,18	29,44
-12,92	0,03	25,68		-13,20	0,02	16,89		-13,19	29,73
-12,92	0,03	25,68		-13,20	0,02	16,89		-13,19	29,73
-13,69	0,03	25,93		-13,29	0,02	16,90		-13,44	29,95
-13,69	0,03	25,93		-13,29	0,02	16,90		-13,44	29,95
-14,28	0,03	26,10		-14,47	0,02	17,11		-14,48	30,20
-14,28	0,03	26,10		-14,47	0,02	17,11		-14,48	30,20
-14,94	0,03	26,26		-14,56	0,02	17,13		-14,70	30,34
-14,94	0,03	26,26		-14,56	0,02	17,13		-14,70	30,34
-15,61	0,03	26,39		-15,73	0,02	17,30		-15,77	30,53
-15,61	0,03	26,39		-15,73	0,02	17,30		-15,77	30,53
-16,18	0,03	26,49		-15,84	0,02	17,31		-15,96	30,62
-16,18	0,03	26,49		-15,84	0,02	17,31		-15,96	30,62
-16,92	0,03	26,59		-16,99	0,02	17,44		-17,06	30,76
-16,92	0,03	26,59		-16,99	0,02	17,44		-17,06	30,76
-17,40	0,03	26,64		-17,11	0,02	17,45		-17,22	30,81
-17,40	0,03	26,64		-17,11	0,02	17,45		-17,22	30,81
-18,22	0,03	26,71		-18,25	0,02	17,54		-18,33	30,91
-18,22	0,03	26,71		-18,25	0,02	17,54		-18,33	30,91
-18,63	0,03	26,74		-18,38	0,02	17,55		-18,49	30,94
-18,63	0,03	26,74		-18,38	0,02	17,55		-18,49	30,94
-19,51	0,03	26,78		-19,50	0,02	17,60		-19,61	31,00
-19,51	0,03	26,78		-19,50	0,02	17,60		-19,61	31,00
-19,85	0,03	26,79		-19,64	0,02	17,60		-19,75	31,01
-19,85	0,03	26,79		-19,64	0,02	17,60		-19,75	31,01
-20,78	0,03	26,80		-20,76	0,02	17,63		-20,88	31,04
-20,78	0,03	26,80		-20,76	0,02	17,63		-20,88	31,04
-21,07	0,03	26,81		-20,91	0,02	17,63		-21,02	31,04
-21,07	0,03	26,81		-20,91	0,02	17,63		-21,02	31,04

-22,05	0,03	26,80		-22,02	0,02	17,62		-22,14	31,03
-22,05	0,03	26,80		-22,02	0,02	17,62		-22,14	31,03
-22,30	0,03	26,79		-22,17	0,02	17,62		-22,29	31,02
-22,30	0,03	26,79		-22,17	0,02	17,62		-22,29	31,02
-23,30	0,03	26,76		-23,28	0,02	17,58		-23,41	30,98
-23,30	0,03	26,76		-23,28	0,02	17,58		-23,41	30,98
-23,52	0,03	26,76		-23,43	0,02	17,57		-23,56	30,97
-23,52	0,03	26,76		-23,43	0,02	17,57		-23,56	30,97
-24,56	0,03	26,71		-24,53	0,02	17,51		-24,67	30,90
-24,56	0,03	26,71		-24,53	0,02	17,51		-24,67	30,90
-24,75	0,03	26,70		-24,69	0,02	17,50		-24,83	30,88
-24,75	0,03	26,70		-24,69	0,02	17,50		-24,83	30,88
-25,80	0,03	26,63		-25,79	0,02	17,41		-25,92	30,78
-25,80	0,03	26,63		-25,79	0,02	17,41		-25,92	30,78
-25,98	0,03	26,61		-25,95	0,02	17,40		-26,11	30,76
-25,98	0,03	26,61		-25,95	0,02	17,40		-26,11	30,76
-27,04	0,03	26,52		-27,05	0,02	17,28		-27,17	30,63
-27,04	0,03	26,52		-27,05	0,02	17,28		-27,17	30,63
-27,22	0,03	26,50		-27,21	0,02	17,26		-27,38	30,60
-27,22	0,03	26,50		-27,21	0,02	17,26		-27,38	30,60
-28,28	0,03	26,39		-28,31	0,02	17,12		-28,42	30,44
-28,28	0,03	26,39		-28,31	0,02	17,12		-28,42	30,44
-28,46	0,03	26,37		-28,47	0,02	17,09		-28,66	30,40
-28,46	0,03	26,37		-28,47	0,02	17,09		-28,66	30,40
-29,51	0,03	26,22		-29,57	0,02	16,92		-29,66	30,20
-29,51	0,03	26,22		-29,57	0,02	16,92		-29,66	30,20
-29,71	0,03	26,19		-29,73	0,02	16,89		-29,94	30,16
-29,71	0,03	26,19		-29,73	0,02	16,89		-29,94	30,16
-30,74	0,03	26,02		-30,83	0,02	16,67		-30,90	29,91
-30,74	0,03	26,02		-30,83	0,02	16,67		-30,90	29,91
-30,96	0,03	25,98		-30,99	0,02	16,64		-31,23	29,86
-30,96	0,03	25,98		-30,99	0,02	16,64		-31,23	29,86
-31,97	0,03	25,78		-32,09	0,02	16,39		-32,14	29,56
-31,97	0,03	25,78		-32,09	0,02	16,39		-32,14	29,56
-32,22	0,03	25,72		-32,24	0,02	16,35		-32,52	29,50
-32,22	0,03	25,72		-32,24	0,02	16,35		-32,52	29,50
-33,19	0,03	25,48		-33,35	0,02	16,05		-33,38	29,15
-33,19	0,03	25,48		-33,35	0,02	16,05		-33,38	29,15
-33,48	0,03	25,39		-33,50	0,02	16,01		-33,82	29,06
-33,48	0,03	25,39		-33,50	0,02	16,01		-33,82	29,06
-34,41	0,03	25,11		-34,62	0,02	15,66		-34,61	28,65
-34,41	0,03	25,11		-34,62	0,02	15,66		-34,61	28,65
-34,76	0,03	24,99		-34,76	0,02	15,61		-35,13	28,53
-34,76	0,03	24,99		-34,76	0,02	15,61		-35,13	28,53
-35,63	0,03	24,66		-35,89	0,02	15,20		-35,84	28,05
-35,63	0,03	24,66		-35,89	0,02	15,20		-35,84	28,05
-36,04	0,03	24,49		-36,01	0,02	15,15		-36,44	27,88
-36,04	0,03	24,49		-36,01	0,02	15,15		-36,44	27,88
-36,86	0,03	24,11		-37,16	0,01	14,68		-37,08	27,34
-36,86	0,03	24,11		-37,16	0,01	14,68		-37,08	27,34
-37,34	0,02	23,86		-37,27	0,01	14,63		-37,77	27,11
-37,34	0,02	23,86		-37,27	0,01	14,63		-37,77	27,11
-38,08	0,02	23,44		-38,43	0,01	14,09		-38,31	26,50
-38,08	0,02	23,44		-38,43	0,01	14,09		-38,31	26,50
-38,66	0,02	23,08		-38,53	0,01	14,04		-39,12	26,16
-38,66	0,02	23,08		-38,53	0,01	14,04		-39,12	26,16
-39,32	0,02	22,62		-39,70	0,01	13,43		-39,56	25,49
-39,32	0,02	22,62		-39,70	0,01	13,43		-39,56	25,49

-40,00	0,02	22,10		-39,80	0,01	13,37		-40,48	25,02
-40,00	0,02	22,10		-39,80	0,01	13,37		-40,48	25,02
-40,56	0,02	21,63		-40,98	0,01	12,68		-40,80	24,30
-40,56	0,02	21,63		-40,98	0,01	12,68		-40,80	24,30
-41,36	0,02	20,90		-41,06	0,01	12,64		-41,86	23,65
-41,36	0,02	20,90		-41,06	0,01	12,64		-41,86	23,65
-41,82	0,02	20,44		-42,27	0,01	11,87		-42,06	22,91
-41,82	0,02	20,44		-42,27	0,01	11,87		-42,06	22,91
-42,77	0,02	19,41		-42,33	0,01	11,82		-43,25	22,02
-42,77	0,02	19,41		-42,33	0,01	11,82		-43,25	22,02
-43,11	0,02	19,02		-43,55	0,01	10,98		-43,32	21,29
-43,11	0,02	19,02		-43,55	0,01	10,98		-43,32	21,29
-44,33	0,02	17,47		-43,61	0,01	10,94		-44,38	19,96
-44,33	0,02	17,47		-43,61	0,01	10,94		-44,38	19,96
-44,53	0,02	17,21		-44,84	0,01	10,04		-44,42	19,31
-44,53	0,02	17,21		-44,84	0,01	10,04		-44,42	19,31
-44,85	0,02	16,77		-44,90	0,01	10,00		-45,30	18,92
-44,85	0,02	16,77		-44,90	0,01	10,00		-45,30	18,92
-45,86	0,02	15,33		-46,12	0,01	9,07		-46,29	17,26
-45,86	0,02	15,33		-46,12	0,01	9,07		-46,29	17,26
-46,79	0,02	13,93		-46,21	0,01	9,00		-46,46	16,05
-46,79	0,02	13,93		-46,21	0,01	9,00		-46,46	16,05
-47,06	0,01	13,52		-47,35	0,01	8,12		-46,63	15,28
-47,06	0,01	13,52		-47,35	0,01	8,12		-46,63	15,28
-47,32	0,01	13,12		-47,53	0,01	7,98		-47,63	14,87
-47,32	0,01	13,12		-47,53	0,01	7,98		-47,63	14,87
-48,24	0,01	11,70		-48,39	0,01	7,31		-48,69	13,35
-48,24	0,01	11,70		-48,39	0,01	7,31		-48,69	13,35
-49,21	0,01	10,23		-48,89	0,01	6,92		-48,82	11,94
-49,21	0,01	10,23		-48,89	0,01	6,92		-48,82	11,94
-49,43	0,01	9,90		-49,35	0,01	6,56		-48,93	11,49
-49,43	0,01	9,90		-49,35	0,01	6,56		-48,93	11,94
-49,64	0,01	9,58		-49,98	0,01	6,08		-49,00	10,98

Figure 43 displays the horizontal soil displacement below the surface. Green line shows the displacement from pile group 1, red line from pile group 2 and the yellow line shows the total displacement after vector addition.

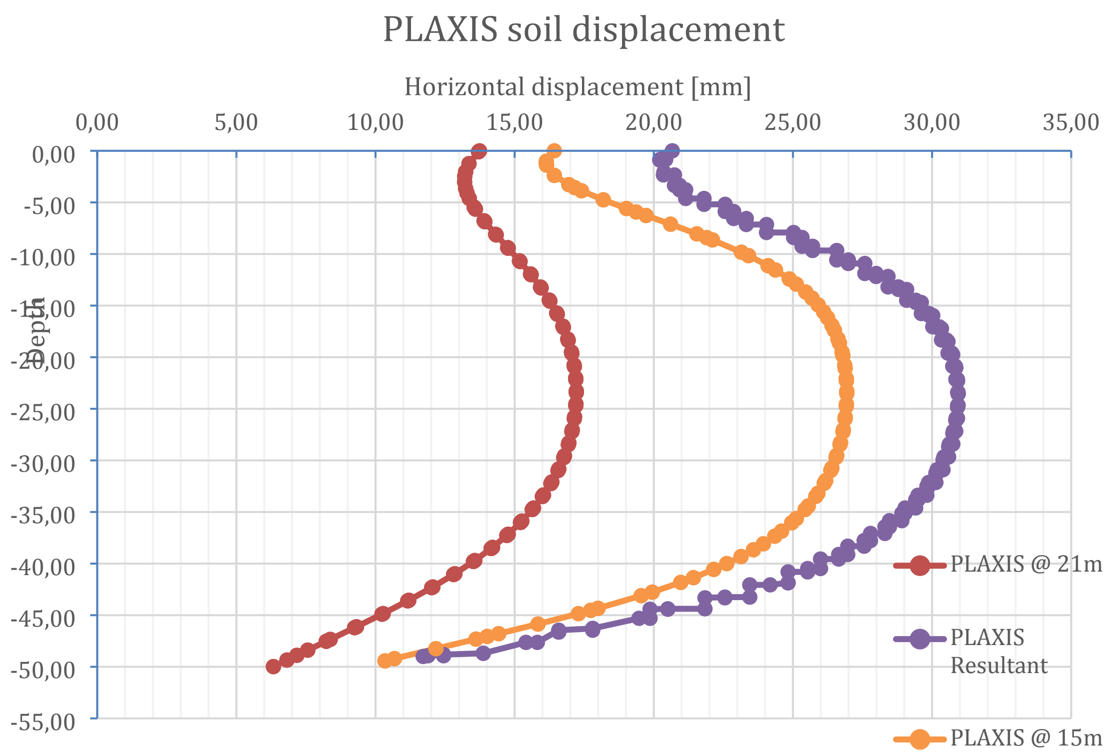

Figure 43. Soil displacement from PLAXIS axisymmetric model